Unexpected roles for AMPK in suppression of autophagy and reactivation of mTORC1 signaling during prolonged amino acid deprivation

Authors: Dubek Kazyken[1*], Sydney G. Dame[1], Claudia Wang[1], Maxwell Wadley[1], and Diane C. Fingar[1*]

Affiliations:
[1]Department of Cell and Developmental Biology
University of Michigan Medical School
Ann Arbor, MI 48109-2200

*Co-corresponding authors: Diane C. Fingar, Ph.D. and Dubek Kazyken, Dept. of Cell and Developmental Biology, University of Michigan Medical School, BSRB #3039, 109 Zina Pitcher Place, Ann Arbor, MI 48109-2200. email: dfingar@umich.edu; dkazyken@umich.edu. Telephone: (734) 763-7541 (dcf office); 734-763-6329 (lab).

ORCID ID: 0000-0002-9801-1482 (DCF)
ORCID ID: 0000-0001-8530-3390 (DK)

Abstract

Amino acid withdrawal suppresses mTORC1 signaling rapidly, which initiates macroautophagy (herein, autophagy). Prolonged amino acid deprivation, however, leads to partial reactivation of mTORC1 due to the liberation of free amino acids by autophagic proteolysis. We observed impaired reactivation of mTORC1 signaling and increased apoptotic cell death upon prolonged amino acid withdrawal in cells lacking the AMPKα1/α2 catalytic subunits. These findings align well with the role of AMPK in promoting cell survival during energetic stress but oppose the well-documented inhibitory action of AMPK toward mTORC1. AMPK-mediated reactivation of mTORC1 during prolonged amino acid deprivation could be explained, however, if AMPK were required for autophagy. Indeed, a prevailing view posits that activation of AMPK by glucose withdrawal promotes autophagy and mitophagy through multisite phosphorylation of ULK1. When we examined the role of AMPK in autophagy induced by amino acid deprivation, however, we found unexpectedly that autophagy remained unimpaired in cells lacking AMPK α1/α2, as monitored by several autophagic readouts in several cell lines. Moreover, the absence of AMPK increased ULK1 signaling, LC3b lipidation, and lysosomal acidity, and the phosphorylation of ULK1 S555 (an AMPK site proposed to induce autophagy) decreased upon amino acid withdrawal or pharmacological mTORC1 inhibition. In addition, activation of AMPK with compound 991, glucose deprivation, or AICAR blunted basal and amino acid withdrawal-induced autophagy. Together our results demonstrate that AMPK suppresses rather than promotes autophagy and supports mTORC1 signaling during prolonged amino acid deprivation, revealing unexpected roles for AMPK in control of these processes.

Keywords:
mTOR; LC3b; ULK1; ATG16L1; compound 991; AICAR glucose deprivation; mTORC2

Abbreviations:
AAs: amino acids; ADP: adenosine diphosphate; AICAR: 5-aminoimidazole-4-carboxamide ribonucleotide; AMP: adenosine monophosphate; AMPK: AMP-activated protein kinase; ATG14: autophagy-related 14; ATG16L1: autophagy-related 16 like 1; ATG5: autophagy-related 5; BafA1: bafilomycin A1; DKD: double knockdown; DKO: double knockout; ECL: enhanced chemiluminescence; LC3b: microtubule-associated proteins 1A/1B light chain 3b; MEFs: mouse embryonic fibroblasts; mTORC1: mechanistic target of rapamycin complex 1; mTORC2: mechanistic target of rapamycin complex 2; p62: ubiquitin-binding protein p62, aka SQSTM1/Sequestosome 1; S6K1 ribosomal protein S6 kinase 1; TEM: transmission electron microscopy; ULK1: Unc-51-like kinase 1; Vps43 vacuolar protein sorting 34.

Introduction

The conserved processes of macroautophagy and selective autophagy (e.g. mitophagy) play important roles in protein quality control [1-3]. During macroautophagy (hereafter referred to as autophagy), bulk cytoplasm containing proteins and organelles become engulfed in a double membrane structure called the autophagosome that fuses with lysosomes to form autolysosomes, which degrade sequestered cargo that can be recycled. A complex set of autophagy (ATG) proteins orchestrates this catabolic response to maintain proteostasis in healthy cells, provide metabolic building blocks during nutrient deprivation, and remove damaged proteins and organelles during stress or disease [1-3]. As such, defective autophagy contributes to various diseases including the neurodegenerative disorders Alzheimer Disease (AD) and Amyotrophic Lateral Sclerosis (ALS), which arise in part due to the accumulation of pathological protein aggregates [4]. Elevated autophagy has also been linked to cancer because it provides metabolites that fuel cell metabolism, growth, and proliferation [4].

mTOR complex 1 (mTORC1) promotes anabolic cellular processes (e.g., ribosomal biogenesis; protein, lipid, and nucleotide synthesis) and suppresses autophagy in nutrient-rich (i.e., presence of amino acids and glucose) and growth factor-rich environments [5-8] by phosphorylating and inhibiting ULK1[9,10] (ATG1 in yeast). As such, amino acid deprivation and the subsequent inactivation of mTORC1 induces autophagy by relieving the suppressive effect of mTORC1 on ULK1 [11-13]. ULK1 nucleates a multi-protein complex that includes ATG13 and FIP200 (FAK family-interacting protein of 200 kDa), which initiates autophagy upon its activation [1-3,14]. The activated ULK1 complex next activates the Vps34 complex, which contains Vps34 (a class III phosphatidylinositol-3-kinase), ATG14, and Beclin-1, through activating phosphorylation of ATG14 and Beclin-1, in part. The Vps34 complex generates PtdIns3P (phosphatidylinositol-3-phosphate) on ATG9-containing membrane vesicles. These vesicles nucleate the formation of double membrane phagophores, which expand around cargo to form mature autophagosomes. PtdIns3P on growing phagophores recruits WIPI2 proteins and ATG16L1-ATG5-ATG12 complexes, which covalently attach LC3 proteins (ATG8 in yeast) to the lipid phosphatidylethanolamine (PE) on growing phagophore membranes, a process known as LC3 lipidation. Indeed, the most widely employed assay for monitoring autophagy measures the conversion of LC3b (LC3b-I) to a lipidated form known as LC3b-II that migrates faster on SDS-PAGE I [15]. This assay can be misinterpreted, however, if not performed rigorously by utilizing autophagic flux inhibitors (e.g., BafA1, an H^+-vATPase inhibitor that maintains an acidic pH within lysosomes, protease inhibitors, or NH_4Cl, which alkalinizes lysosomes) [15,16]. These flux inhibitors blunt late-stage autophagic proteolysis of lipidated LC3-II and autophagy receptors such as p62/SQSTM1 by acid-loving proteases, thus enabling an accurate assessment of LC3b-II and p62/SQSTM1 levels in the absence of degradative flux [15].

In addition to amino acid deprivation, a fall in cellular energy levels (i.e., a rise in the AMP to ATP ratio) caused by prolonged glucose deprivation or mitochondrial poisons inhibits mTORC1 signaling by activating AMPK (AMP-activated protein kinase) (Snf1p in yeast) [11,17-23]. Mild glucose withdrawal can also activate AMPK in an ATP-independent manner to inhibit mTORC1 [24]. AMPK activation redirects cell metabolism away from mTORC1-mediated, ATP-consuming anabolic processes and toward ATP-generating, catabolic processes (e.g., fatty acid oxidation; glucose uptake; lysosomal and mitochondrial biogenesis) that in turn balance energy supply and demand and therefore promote cell survival [11,20,21,23]. AMPK functions as a heterotrimer composed of a catalytic α-subunit (α1 or α2) and regulatory β- and γ-subunits (β1 or β2; γ1, γ2, or γ3) [20,21,23]. Due to its heterotrimeric assembly and multiple subunits, AMPK potentially assembles into 12 distinct isoforms [20,21,23]. As the subunits display tissue-specific expression, most cells express only a subset of these 12 $AMPK_{\alpha\beta\gamma}$ isoforms, however [21]. During energetic stress, AMP (or ADP) binds to the γ-subunit, leading to a conformational change that increases the phosphorylation of the catalytic AMPK α-subunit on its essential activation loop site (T172) by LKB1 or the Ca^{2+}-sensitive kinase CaMKKβ [20,21,23].

A widely accepted model proposes that activation of AMPK by glucose deprivation induces autophagy and mitophagy through multi-site phosphorylation of ULK1 and Beclin-1 [2,3,9,23,25-30]. In this model, mTORC1 phosphorylates ULK1 S757 (human S758) in complete media containing glucose and amino acids, which destabilizes a complex between AMPK and ULK1, thereby reducing AMPK-mediated phosphorylation and activation of the ULK1 [25]. Conversely, the model proposes that activation of AMPK with glucose withdrawal reduces mTORC1-mediated phosphorylation of ULK1 S757, which stabilizes the AMPK-ULK1 complex, thus enabling AMPK to phosphorylate ULK1 on several sites, resulting in the initiation of autophagy [25,26]. These findings have led to the widely accepted idea that AMPK promotes autophagy [2,3,23,31]. It is important to note, however, that several studies have questioned aspects of this model. For example, several studies found that glucose withdrawal failed to induce autophagy in mammalian cells and yeast [32-34] while glucose withdrawal suppressed autophagy induced by amino acid withdrawal [34]. In addition, the withdrawal of amino acids or pharmacological inhibition of mTORC1, conditions that induce autophagy, was shown to destabilize the AMPK-ULK1 complex and reduce the phosphorylation of ULK1 S555 [34,35], a site phosphorylated by AMPK and proposed to induce autophagy [26,29]. Thus, a conundrum exists regarding the role of glucose deprivation and its activation of AMPK in the control of autophagy. Due to the interest in AMPK as a therapeutic drug target for several chronic diseases (e.g., type II diabetes) and its dual role as a tumor suppressor or promoter depending on cellular context [21,36-41]**,** it is critical to clarify the role of AMPK in autophagy.

In this study, we examined how AMPK controls autophagy during amino acid deprivation. Using multiple orthogonal assays of autophagy in several cell types, we found unexpectedly that autophagy induced by amino acid withdrawal or mTORC1 inhibition occurred unimpaired in cells with double knockout (DKO) or double knockdown (DKD) of AMPKα1 and α2. More surprisingly, the absence of AMPK increased basal and amino acid withdrawal-induced autophagy while the activation of AMPK suppressed autophagy. Thus, AMPK suppresses autophagy in the context of amino acid deprivation, a finding that challenges the prevailing view that AMPK promotes autophagy. It is important to note that we initiated this study in response to another unexpected observation. We observed that the reactivation of mTORC1 signaling following prolonged amino acid deprivation was impaired in cells lacking AMPKα1 and α2. While acute amino acid withdrawal inhibits mTORC1 rapidly (30-60 minutes) due to its dissociation from Rag GTPases on lysosomal membranes, where an important activator, Rheb, resides [6,7,42-44], mTORC1 re-activates partially at later time points (1-2 hours and more) due to the induction of autophagy and the subsequent liberation of free amino acids by autophagic proteolysis [11,45-47]. This reactivation of mTORC1 limits the extent of autophagy and enables the regeneration of lysosomes, a process known as ALR (autophagic lysosome regeneration) [45,48]. At first glance, the AMPK-dependent reactivation of mTORC1 opposed the role of AMPK as an inhibitor of mTORC1. On second thought, however, it made sense, due to the widely accepted view that AMPK promotes autophagy, at least during glucose deprivation [2,3,23,31]. We presumed that the impaired reactivation of mTORC1 signaling during prolonged amino acid deprivation in AMPKα DKO cells was a secondary consequence of impaired autophagy. This presumption proved incorrect, however, as we found that AMPK inhibits autophagy. Thus, AMPK supports mTORC1 signaling during amino acid deprivation by a new albeit unknown mechanism. In summary, this study forces a reexamination of the role of AMPK in autophagy-linked cell physiology and disease and reveals context-dependent regulation of mTORC1 by AMPK.

Results

AMPK suppresses apoptotic cell death and promotes the reactivation of mTORC1 signaling during prolonged amino acid deprivation

mTORC1 and mTOR complex 2 (mTORC2) respond to diverse stimuli, including growth factors, hormones, and cell stress [6,49,50]. Upon activation, the mTORC1 pathway promotes anabolic cellular

processes and suppresses autophagy while the mTORC2 pathway controls Akt-dependent cell metabolism and promotes cell survival. mTORC1 but not mTORC2 signaling requires a sufficient level of amino cellular amino acids, which are sensed by the Ragulator (LAMTOR)-Rag GTPase pathway [6,7,42,43,51]. Our prior work demonstrated that AMPK directly activates mTORC2 through phosphorylation of mTORC2 components, which promotes cell survival during energetic stress [52]. We were therefore curious as to whether AMPK also promotes cell survival during amino acid deprivation, a different type of nutrient stress. We, therefore, examined how amino acid withdrawal for 0.5-16 hr affects apoptosis in MEFs and HeLa cells containing or lacking the AMPK catalytic subunits, AMPKα1 and AMPKα2. Markers of apoptosis (i.e., cleavage of PARP or caspase 3) increased modestly in wild type cells at 8-16 hr of amino acid withdrawal but increased strongly in AMPKα DKO cells (Fig. 1A, 1B). AMPKα DKO MEFs displayed reduced cell viability upon amino acid withdrawal for 16 hr (Fig. 1C, 1D). AMPKα DKO MEFs also displayed reduced mTORC2-dependent Akt S473 phosphorylation across the time course (Fig. 1E), which likely explains their elevated apoptosis during amino acid deprivation compared to wild type MEFs. mTORC2-Akt signaling in HeLa cells was less dependent on AMPK, however (Fig. 1F). These results demonstrate that AMPK protects against cell death during nutrient stress caused by amino acid deprivation, like its protective role during energetic stress [53].

We next examined how amino acid withdrawal affects mTORC1 signaling in wild type vs. AMPKα DKO MEFs and HeLa cells. As expected, the acute removal of amino acids from wild type MEFs for 0.5 hr reduced mTORC1 signaling, as monitored by the phosphorylation of S6K1 T389, and mTORC1 signaling reactivated partially at later time points, increasing as early as 1 hr after amino acid withdrawal and increasing further at 2-6 hr (Fig. 1E). HeLa cells responded similarly but with slightly slower kinetics (Fig. 1F). These observations agree with prior studies demonstrating that prolonged amino acid deprivation leads to the partial reactivation of mTORC1 signaling due to the induction of autophagy and the liberation of free amino acids [11,45-47]. Indeed, we confirmed that autophagic proteolysis in part underlies the reactivation of mTORC1 signaling following prolonged amino acid deprivation. Pretreating MEFs or HeLa cells with BafA1 led to the accumulation of lipidated LC3b-II in the basal state (i.e., in complete media) and amino acid-deprived state and blunted the reactivation of mTORC1 (Fig. 1G, 1H). Somewhat surprisingly, we found that mTORC1 reactivation was impaired in AMPKα DKO MEFs and HeLa cells relative to control cells (Fig. 1E; 1F). While at first glance this result was unexpected due to the established role of AMPK as a suppressor of mTORC1 (at least during energetic stress) [17,18,20], it made sense considering the prevailing view that AMPK promotes autophagy (at least during glucose deprivation) [2,3,25,26,30]. Thus, we presumed that the impaired reactivation of mTORC1 signaling during prolonged amino acid deprivation resulted from an insufficient level of autophagic proteolysis. At this point, we decided to examine how AMPK controls autophagy during amino acid deprivation to understand why AMPK is required for optimal mTORC1 reactivation in the prolonged absence of amino acids. The following results demonstrate that AMPK suppresses rather than promotes autophagy in the context of amino acid deprivation. Therefore, AMPK supports mTORC1 signaling during amino acid deprivation not by promoting autophagy but by a new albeit unknown mechanism (Fig. 1I).

The absence of AMPK increases basal and amino acid withdrawal-induced autophagy

We tested whether the induction of autophagy in response to amino acid deprivation requires AMPK by studying AMPKα DKO MEFs and other DKO cell lines (i.e., HeLa; HEK293; U2OS) as well as C2C12 cells with acute siRNA-mediated double knockdown (DKD) of AMPKα1/α2. To monitor autophagy, we employed several assays including the lipidation of LC3b, the induction of LC3b and p62 puncta microscopically, and the phosphorylation of ATG16L1 S278, a site phosphorylated directly by ULK1 on newly forming autophagosomes that correlates well with autophagic rate [54]. We also used transmission electron microscopy (TEM) to visually observe the formation of autophagosomal- and autolysosomal-like structures. Importantly, when measuring LC3b lipidation, the induction of LC3b and p62 puncta, or the

formation of autophagosomes and autolysosomes by TEM in response to amino acid withdrawal, we pretreated cells with BafA1 to suppress autophagic proteolysis. Since ATG16L1 S278 phosphorylation is not influenced by autophagic degradation [54], we analyzed ATG16L1 P-S278 in the absence of BafA1. To monitor AMPK activity, we measured the phosphorylation of ULK1 S555, a site phosphorylated directly by AMPK and proposed to induce autophagy. To perform the amino acid withdrawal experiments in this study, we first refed cells with DMEM/FBS [10%] for 1 hr. We then washed and refed the cells with precisely matched amino acid replete (i.e., complete media) or amino-acid free DMEM containing dialyzed FBS and glucose (see Materials and Methods for more details). We therefore used identical media containing glucose and serum growth factors, which contained or lacked only amino acids, for the experiments in this study.

In wild type MEFs and C2C12 cells, amino acid withdrawal for 1-4 hours induced the accumulation of LC3b-II in the presence of BafA1, and amino acid withdrawal increased the phosphorylation of ATG16L1 S278 in both the absence and presence of BafA1, as expected (Fig. 2A, 2B). In AMPKα DKO MEFs and AMPKα DKD C2C12 cells, the absence of AMPKα ablated or reduced ULK1 S555 phosphorylation, respectively, demonstrating functional inactivation of AMPK (Fig. 2A, 2B). Unexpectedly, LC3b-II (normalized to tubulin) accumulated to a similar level in amino acid deprived wild type vs. AMPKα DKO MEFs and in control vs. AMPKα DKD C2C12 cells treated with BafA1 (Fig. 2A, 2B). In addition, ATG16L1 P-S278 was higher (not lower) in AMPKα DKO/DKD cells relative to control cells in the absence of BafA1 (Fig. 2A, 2B). These data indicate that the induction of autophagy occurs unimpaired in MEFs and C2C12 cells lacking AMPK. Moreover, the elevation of ATG16L1 P-S278 suggested that AMPKα DKO/DKD increases the initiation of autophagy induced by amino acid withdrawal. As a control, we examined MEFs lacking ATG5, an essential autophagy protein important for the lipidation of LC3b. ATG5 knockout ablated the formation of LC3b-II and the phosphorylation of ATG16L1, as expected (Fig. S1A). Importantly, when we used a different method to blunt autophagic flux, i.e., the lysosomal protease inhibitors E64D plus pepstatin A, we found that LC3b-II accumulated similarly in wild type and AMPKα DKO MEFs (Fig. S1B).

To study the role of AMPK in control of autophagy more rigorously, we compared autophagic responses quantitatively in several different cell lines cultured in complete media vs. amino acid-free media for 2 hr in the presence of BafA1. Consistent with the time course results, amino acid deprivation induced the accumulation of LC3b-II (normalized to α-tubulin) to a statistically similar extent in wild type vs. AMPKα DKO MEFs and in control vs. AMPKα DKD C2C12 cells (Fig. 2C, 2D, 2E, 2F), indicating that AMPK is not required for autophagy induced by amino acid deprivation. We obtained similar results in CRISPR/Cas9-engineered MEFS, C2C12, HeLa, HEK293, and U2OS cells lacking AMPKα1 and α2 (Fig. S2A, S2B; S2C, S2D, S2E). Finding that results obtained from newly generated MPKα1/α2 DKO MEFs phenocopied those from the AMPKα1/α2 DKO MEFs generated over a decade ago from transgenic mice [55] reassures us that the ability of AMPKα double knockout to increase autophagy results not from cellular rewiring due to chronic inactivation of an important protein (i.e., AMPK) but from the loss of AMPK.

We next quantitated LC3b-II accumulation by normalizing LC3b-II to LC3b-I. It is important to note that upon induction of autophagy and lipidation of LC3b, levels of non-lipidated LC3b-I (upper band) decrease with corresponding increases in lipidated LC3b-II (lower band). The ratio of LC3b-II/LC3b-I (in the presence of BafA1) thus discriminates better between the induction of autophagy vs. a block in late-stage autophagic flux than normalizing LC3b-II to α-tubulin [15]. We found that LC3b-II/LC3b-I ratios were significantly higher in both complete media and amino acid-free media in AMPKα DKO MEFs and AMPKα DKD C2C12 cells relative to controls (Fig. 2D, 2F). When we monitored ULK1 signaling by measuring ATG16L1 S278 phosphorylation quantitatively, we found that AMPKα DKO MEFs and AMPKα DKD C2C12 cells displayed significantly higher ATG16L1 P-S278 relative to control cells upon amino acid withdrawal (Fig. 2C, 2D, 2E, 2F). In the basal state (i.e., in complete media), C2C12 cells but

not MEFs lacking AMPK displayed significantly elevated ATG16L1 P-S278 (Fig. 2D, 2F). To complement our experiments utilizing genetic AMPK inactivation, we used the AMPK inhibitor BAY-3827 [56], which likely has improved specificity for AMPK than compound C, an AMPK inhibitor notorious for many AMPK-independent off-target effects [40]. We found that treatment of MEFs with BAY-3827 had no negative impact on the accumulation of LC3b-II or the phosphorylation of ATG16L1 P-S278 during amino acid deprivation (Fig. S2F).

We next examined levels of p62/SQSTM1, an autophagy receptor that links cargo to growing phagophore membranes and becomes degraded by late-stage autophagic proteolysis [57]. We found that the degradation of p62 upon amino acid withdrawal was not impaired by the absence of AMPK in MEFs or C2C12 cells relative to controls (Fig. 2G, 2H). In addition, basal p62 expression was lower in AMPKα DKD C2C12 cells relative to control cells, likely due to increased basal autophagic proteolysis (see Fig. 2E, 2F). To quantitate the rate of autophagic flux, we measured the fold change of LC3b-II/α-tubulin +BafA1/-BafA1 (i.e., the rate of LC3b turnover/degradation). Not only was amino acid withdrawal-induced autophagic flux not impaired in AMPKα DKO MEFs or DKD C2C12 cells, the absence of AMPK increased autophagic flux significantly in the basal state and in the amino acid-deprived state in both cell lines (Fig. S2G, S2H). Together these results indicate that basal autophagy and autophagy induced by amino acid withdrawal occur more readily in the absence of AMPK, suggesting that AMPK exerts a suppressive effect on autophagy during amino acid deprivation.

AMPK is not required for autophagy induced by pharmacological mTORC1 inhibition

Inhibition of mTORC1 by pharmacological agents induces autophagy to different extents depending on the type of inhibitor and cell type. For example, in most cell types, the active site mTOR inhibitor Torin1 induces autophagy robustly due to complete inhibition of mTORC1 while the allosteric inhibitor rapamycin induces autophagy weakly if at all [58,59]. To test whether AMPK is required for induction of autophagy during pharmacological mTORC1 inhibition, we treated wild type and AMPKα DKO MEFs and AMPKα DKD C2C12 cells with Torin1 for 1-4 hr and monitored autophagy in the absence and presence of BafA1. As expected, Torin1 reduced mTORC1 signaling strongly (as measured by S6K1 P-T389 and ULK1 P-S757) and induced a time-dependent accumulation of LC3b-II in BafA1 treated cells (Fig. 3A, 3B). Torin1 increased LC3b-II levels similarly in BafA1-treated cells lacking AMPKα relative to controls, indicating that AMPK is not required for Torin1-induced autophagy (Fig. 3A, 3B, 3C, 3D). While Torin1 increased ATG16L1 P-S278 similarly in wild type and AMPKα DKO MEFs in the absence of BafA1 (Fig. 3A, 3C), AMPKα DKD C2C12 cells displayed higher levels of ATG16L1 P-S278 relative to controls, suggesting elevated ULK1 signaling and accelerated initiation of autophagy (Fig. 3B, 3D). Interestingly, like amino acid withdrawal, Torin1 reduced the phosphorylation of ULK1 on the AMPK site (i.e., S555) in both MEFs and C2C12 cells (Fig. 3A, 3B). In addition, AMPK was not required for Torin1-induced autophagy in HeLa or HEK293 cells (Fig. S3A, S3B. We also confirmed that ATG5 KO MEFs display complete resistance to Torin1-induced autophagy (Fig. S3D). Together these results demonstrate that Torin1-induced autophagy occurs unimpaired in the absence of AMPK.

Formation of autophagosomal- and autolysosomal-like structures by amino acid deprivation occurs unimpaired in cells lacking AMPK, with evidence of increased autophagy

We next monitored the formation of endogenous LC3b puncta, ATG16L1-S278 puncta, and p62 puncta by confocal immunofluorescence. Upon initiation of autophagy, lipidated LC3b concentrates on newly forming phagophore membranes that expand and mature into autophagosomes that appear as puncta by microscopy. Amino acid withdrawal increased the number of LC3b puncta in MEFs and C2C12 cells containing or lacking AMPK and treated with BafA1 (Fig. 4A-4D). In C2C12 cells but not MEFs, AMPKα DKD increased LC3b puncta number during amino acid deprivation relative to controls (Fig. 4E, 4F). Puncta containing phosphorylated ATG16L1 S278 also form on phagophore membranes during amino acid

deprivation in mammalian cells [54]. Like LC3b staining, amino acid withdrawal increased ATG16L1 P-S278 puncta in MEFs and C2C12 cells in the presence and absence of AMPK (Fig. 4E-4H). In MEFs but not C2C12 cells, AMPKα DKO increased ATG16L1 P-S278 puncta during amino acid deprivation relative to control cells (Fig. 4C, 4D). We next monitored p62/SQSTM1 puncta, which form due to the recruitment of p62/SQSTM1 to phagophore membranes after the initiation of autophagy [57]. Upon withdrawal of amino acids in the presence of BafA1, p62/SQSTM1 puncta number was significantly higher in AMPKα DKO MEFs relative to wild type MEFs (Fig. 4J). Transmission electron microscopy (TEM), the original method for monitoring autophagy, enables one to visually observe the formation of autophagosomes and autolysosomes upon the withdrawal of amino acids. We found that the ability of amino acid withdrawal to increase the number of autophagosomal- and autolysosomal-like structures was not impaired in AMPKα DKO MEFs or AMPKα DKD C2C12 cells relative to control cells (Fig. 5A-5D). Moreover, AMPKα DKO MEFs (but not AMPKα DKD C2C12 cells) displayed higher numbers of these structures upon amino acid withdrawal relative to control cells (Fig. 5A-5B). Together these results demonstrate that AMPK is not required for the formation of autophagosomes and autolysosomes upon amino acid deprivation, with evidence of increased autophagy in the absence of AMPK.

Activation of AMPK suppresses autophagy induced by amino acid deprivation

To strengthen our findings that the absence of AMPK accelerates autophagy, we examined how the activation of AMPK affects basal and amino acid withdrawal-induced autophagy. To do so, we employed different agents to activate AMPK including the pharmacological agonist compound 991, glucose deprivation, or AICAR (an AMP mimetic compound). In MEFs and C2C12 cells treated with BafA1, compound 991 reduced the accumulation of LC3b-II significantly in response to amino acid withdrawal in an AMPK-dependent and statistically significant manner (Fig. 6A-6D). In the basal state, 991 also reduced the accumulation of LC3b-II significantly in both cell types (Fig. S4A, S4B). While the LC3b-II lowering effect of 991 on basal autophagy was AMPK dependent in MEFs, it was not wholly dependent on AMPK in C2C12 cells, likely due to incomplete siRNA-mediated knockdown of AMPKα1/α2. In HEK293 cells, 991 also reduced the accumulation of LC3b-II in the basal and amino acid-deprived states in an AMPK-dependent manner (Figure S4C). As expected, 991 increased ULK1 S555 phosphorylation in MEFs, C2C12 cells, and HEK293 cells, indicating increased AMPK activity (Fig. 6A, 6C, S4C). We next examined the formation of LC3b puncta microscopically. Compound 991 reduced the number of LC3b puncta induced by amino acid withdrawal significantly in BafA1-treated MEFs and C2C12 cells (Fig. 6E-6H). These results demonstrate that the activation of AMPK by 991 suppresses autophagy induced by amino acid deprivation in an AMPK-dependent manner.

To increase AMPK activity more physiologically, we glucose-deprived cells. In agreement with results obtained using compound 991, withdrawal of glucose for 2 hr from MEFs and C2C12 cells treated with BafA1 suppressed the ability of amino acid withdrawal to induce the accumulation of LC3b-II to a significant extent in an AMPK-dependent manner (Figures 7I-7L). Furthermore, glucose starvation alone (i.e., in the presence of amino acids) failed to increase the conversion of LC3b-I to LC3b-II in wild type MEFs and C2C12 cells, indicating that glucose deprivation does not induce autophagy, thus opposing the prevailing view that glucose deprivation induces autophagy (Fig. S4D, S4E). Curiously, glucose withdrawal accelerated the conversion of LC3b-I to LC3b-II significantly in AMPKα DKO MEFs (but not C2C12 cells) (Fig. S4D, S4E), suggesting that glucose deprivation can accelerate autophagy in the absence of the suppressive effect of AMPK, at least in MEFs. In agreement, Williams et al. noted that shifting AMPKα DKO from high to low glucose induced the formation of LC3 puncta [60]. We also used AICAR to activate AMPK. Like experiments using compound 991 or glucose withdrawal, AICAR suppressed both basal and amino acid withdrawal-induced accumulation of LC3b-II in an AMPK-dependent manner (Figure S4F), which supports a prior study demonstrating that AICAR suppresses autophagy in rat hepatocytes [61]. Together our results reveal that AMPK activation suppresses autophagy induced by amino acid withdrawal.

Activation of AMPK suppresses ULK1 signaling and lysosomal acidification induced by amino acid deprivation

We next explored the mechanism by which AMPK suppresses autophagy. During amino acid sufficiency, mTORC1 phosphorylates ULK1 S757 (human S758), which suppresses the activity of the autophagy initiating ULK1 complex [2,3,10,25]. Amino acid deprivation therefore initiates autophagy by relieving the suppressive effect of mTORC1 on ULK1. The activated ULK1 complex phosphorylates downstream substrates, including ATG16L1, a component of the LC3b lipidation machinery, and ATG14 and Beclin1, components of the Vps34 complex [2,3]. Amino acid deprivation also acidifies lysosomes, which occurs in a ULK1-independent manner [34], to facilitate autophagic degradation within autolysosomes. As we found that the absence of AMPK increased ATG16L1 S278 phosphorylation during amino acid deprivation in several cell types (see Fig. 2C-2F; S2A-F), we next examined how activation of AMPK with compound 991, glucose deprivation, or AICAR affects the activity of the ULK1 complex by measuring ATG16L1 P-S278 in the basal and amino acid-deprived states in the absence of BafA1. We found that compound 991 suppressed the ability of amino acid withdrawal to increase ATG16L1 P-S278 significantly in an AMPK-dependent manner in MEFs (Fig. 7A-7B) and C2C12 cells (Fig. 7C-7D). Compound 991 also reduced P-ATG16L1 S278 significantly in the basal state in both cell types (Fig. S4A, S4B), although the reduction in P-ATG16L1 mediated by 991 in C2C12 cells was not wholly AMPK dependent, likely due to incomplete knockdown of AMPKα1 and α2. Importantly, we confirmed the dependency of ATG16L1 P-S278 on ULK1 activity. Pretreating MEFs with the ULK1 inhibitor MRT-68921 (Fig. 7E, 7F) or knocking out ULK1 and its homologue ULK2 from MEFs (Fig. S5) ablated ATG16L1 P-S278. These results confirm that the ATG16L1 P-S278 antibody indeed monitors ULK1 activity. Like compound 991, glucose withdrawal suppressed the ability of amino acid withdrawal to increase ATG16L1 P-S278 in an AMPK-dependent and significant manner in MEFs (Fig. 7G-7H) and C2C12 cells (Fig. 7I-7J). These results demonstrate that AMPK suppresses ULK1 signaling induced by amino acid deprivation.

As Nwadike et al. found that activation of AMPK with A-769662 suppressed the acidification of lysosomes mediated by amino acid withdrawal [34], we next examined lysosomal acidification in wild type vs. AMPKα DKO MEFs and in control vs. AMPKα DKD C2C12 cells by staining cells with LysoTracker, a cell-permeable, pH-sensitive dye that fluoresces more strongly in an acidic environment. In agreement with Nwadike et al., we confirmed that amino acid withdrawal increased LysoTracker staining in MEFs and C2C12 cells. We also found that absence of AMPK increased this staining in both complete and amino acid-free media in a statistically significant manner (Fig. 7K-7N). These results confirm that AMPK suppresses lysosomal acidification in both the basal and amino acid-deprived states.

Activation of AMPK suppresses autophagic initiation and progression induced by pharmacological mTORC1 inhibition

We next tested how activation of AMPK with compound 991 affects autophagy induced by pharmacological mTORC1 inhibition compared to that induced by amino acid withdrawal. In complete media, Torin1 increased LC3b-II levels and ATG16L1 S278 phosphorylation to a level similar to or higher than that obtained in amino acid-free media, as expected (Fig. 8A-8D). Treatment with 991 attenuated the Torin1-induced increases in LC3b-II and ATG16L1 P-S278 significantly (Fig. 8A-8D). Compound 991 also suppressed the rapamycin-induced effects on autophagy, although rapamycin was less effective at inducing autophagy than Torin1, particularly in C2C12 cells (Fig. 8A-8D). We next asked whether 991 attenuates Torin1-induced autophagy in an AMPK-dependent manner. Compound 991 failed to reduce Torin1-induced LC3b-II accumulation or ATG16L1 P-S278 in AMPKα DKO MEFs or AMPKα DKD C2C12 cells cultured in complete media with BafA1 (Fig. 8E, 8F). These results indicate that activation of AMPK suppresses ULK1 kinase activity and autophagic progression induced by pharmacological

mTORC1 inhibition (Fig. 8G). Interestingly, we also observed that Torin1 or rapamycin treatment attenuated the suppressive effect of 991 on basal and amino acid withdrawal-induced autophagy (Figures 8A, 8C). These observations support a model whereby mTORC1 and AMPK each suppress autophagy by independent mechanisms operating in parallel (Figure 8G).

AMPK supports mTORC1 signaling during prolonged amino acid deprivation

We launched this investigation into the role of AMPK in control of autophagy upon observing impaired reactivation of mTORC1 signaling upon prolonged amino acid deprivation in cells lacking AMPK (see Fig. 1D; 1E). Our results described above reveal that AMPK suppresses rather than promotes autophagy during prolonged amino acid deprivation. Therefore, AMPK supports the reactivation of mTORC1 signaling during amino acid deprivation not by promoting autophagy but by some other mechanism. This finding opposes the established view that AMPK inhibits mTORC1 in general. We next sought to quantify the supportive effect of AMPK on mTORC1 signaling during prolonged amino acid deprivation. As shown in Figures 9A and 9B, double knockout of AMPKα1/α2 from MEFs reduced S6K1 T389 phosphorylation significantly upon removal of amino acids for 2 and 4 hr relative to wild type MEFs (see also Fig. 1E, 2A, 2C, 7A, 7C, 7G; no BafA1 treatment). We also noted throughout this study that the absence of AMPK reduced ULK1 S757 phosphorylation. Chronic double knockout of AMPKα also reduced total levels of ULK1, however, thus rendering it uncertain as to whether the absence of AMPK truly reduces ULK1 P-S757 by quick visual inspection of blots. Thus, it was critical to normalize ULK1 P-S757 to total ULK1. We found that double knockout of AMPKα from MEFs reduced mTORC1-mediated ULK1 P-S757 significantly (Fig. 1A, 1B). We next quantified the support of mTORC1 signaling by AMPK in HeLa cells deprived of amino acids. As shown in Figures 9C and 9D, double knockout of AMPKα1/α2 from HeLa cells also reduced S6K1 T389 and ULK1 S757 phosphorylation significantly upon removal of amino acids for 4 hr relative to control cells. In complete media, AMPKα DKO from HeLa cells but not MEFs reduced mTORC1 signaling to S6K1 modestly but significantly (Fig. 9B, 9D). These results demonstrate that AMPK supports mTORC1 signaling during prolonged amino acid deprivation.

mTORC1 positively controls AMPK-mediated ULK1 phosphorylation

Throughout this study, we also noted that amino acid withdrawal (see Fig. 2, S2, and others) or Torin1 treatment (see Fig. 3 and 8) reduced the phosphorylation of ULK1 S555, a site phosphorylated by AMPK and proposed to initiate autophagy, in several cell types. Earlier work by other groups made similar observations [34,35]. When we quantified the effect of amino acid levels on ULK1 S555 phosphorylation in MEFs and C2C12 cells, amino acid withdrawal indeed reduced ULK1 P-S555 significantly (Fig. 9E). We also normalized P-ULK-S555 to α-tubulin rather than to total ULK1, because ULK1 downshifts on SDS-PAGE in the absence of amino acids, likely due to reduced phosphorylation, generating a darker ULK1 band that when quantified would erroneously increase the fold reduction of ULK1 P-S555 caused by amino acid withdrawal. After normalizing P-ULK-S555 to α-tubulin, amino acid withdrawal still decreased ULK P-S555 to a significant degree (Fig. 9F). As expected, double knockout of AMPKα from MEFs or double knockdown of AMPKα from C2C12 cells ablated or reduced ULK1 P-S555, respectively (see Fig. 2A, 2B, 2C, 2E plus others), while AMPK activation with compound 991 increased ULK1 P-S555, albeit modestly (see Fig. 6A, 6C, 7C, 7E). Since amino acid withdrawal or Torin1 reduced ULK1 P-S555, we were curious as to how acute amino acid stimulation would affect ULK1 P-S555. The addition of amino acids for 10 minutes to cells deprived of amino acids for 50 minutes increased ULK1 P-S555 in an AMPK-dependent and Torin1-sensitive manner (Fig. 9G, 9H). As expected, amino acid stimulation increased S6K1 P-T389 and ULK1 P-S757. These results indicate that mTORC1 activity positively controls the ability of AMPK to phosphorylate ULK1 S555.

Discussion

AMPK functions canonically as a conserved sensor of energetic stress that balances energy supply and demand and therefore promotes cell survival [20,21,23]. The prevailing view that AMPK promotes autophagy or mitophagy during glucose deprivation [9,25,26,29,30] fits well with these canonical functions of AMPK. Consistently, we found that cells lacking AMPK displayed increased apoptosis during nutrient stress caused by amino acid withdrawal (see Fig. 1A, 1B). However, our work challenges the view that AMPK promotes autophagy, an idea that has gained popularity over the last decade [2,3,23,31] since the discovery that AMPK phosphorylates ULK1 and Beclin-1 directly [25-27]. We found that AMPK suppresses autophagy in the basal and amino acid-deprived states, likely through AMPK-mediated phosphorylation of ULK1 and other autophagy proteins (Fig. 10A). Upon withdrawal of amino acids, the absence of AMPK increased ULK1 signaling to ATG16L1 and the lipidation of LC3b; conversely, activating AMPK using several methods suppressed these readouts **(**Fig. 10A). As autophagy is an energetically costly process [62,63], finding that AMPK limits autophagy aligns well with the canonical role of AMPK in the suppression of ATP-consuming processes. AMPK-mediated suppression of autophagy would thus enable the remaining minimal levels of metabolites and energy reserves to support essential cellular processes. Interestingly, Kim et al. presented supplementary data showing that upon the withdrawal of amino acids, LC3b-II accumulated to a higher level in AMPKα DKO MEFs relative to wild type MEFs treated with NH_4Cl , a flux inhibitor [25]. While these results were not quantified, they suggested that AMPK suppressed autophagy during amino acid deprivation, consistent with our results here. For reasons that remain unclear, the significance of this observation was not embraced, and the concept that AMPK promotes autophagy has become the accepted view. We also confirmed that AMPK suppresses the acidification of lysosomes induced by amino acid withdrawal, in agreement with Nwadike et al. **(**Fig. 10A) [34]. Thus, AMPK suppresses autophagy by at least two mechanisms, by reducing ULK1 complex activity and by blunting lysosomal acidification.

The model that glucose deprivation induces autophagy and mitophagy through AMPK-mediated multisite phosphorylation of ULK1 [25,26,29,30] makes physiological sense, as such a response would generate metabolites, thus improving cellular bioenergetics and enhancing cell survival. However, we and other groups [32-34] found that glucose withdrawal failed to induce the accumulation of LC3b-II in cells treated with a flux inhibitor, and glucose withdrawal suppressed the induction of autophagy upon amino acid withdrawal [34]. Furthermore, several earlier studies have questioned the importance of AMPK in the induction of autophagy. For example, activation of AMPK with AICAR or with the mitochondrial poisons phenformin or metformin either suppressed autophagy or had no effect [61,64]. Double knockout of AMPKα1/α2 from MEFs treated with a flux inhibitor increased levels of LC3b-II in the basal state and upon induction of autophagy by serum deprivation relative to control cells [60]. Phosphorylation of both ATG13 S258 and S224 by mTORC1 and AMPK, respectively, suppressed ULK1 signaling and the accumulation of LC3b-II during amino acid deprivation, suggesting that AMPK, like mTORC1, suppresses autophagy [65]. Therefore, abundant evidence suggests that glucose deprivation and AMPK activation does not induce autophagy. The reasons underlying the discrepant results regarding control of autophagy in glucose-deprived conditions remain unclear. Future work, however, warrants further investigation into the role of AMPK in mitophagy during glucose deprivation.

We and other groups found that amino acid withdrawal or pharmacological mTORC1 inactivation paradoxically reduced (rather than increased) phosphorylation of ULK1 S555 [34,35], an AMPK site proposed to induce mitophagy upon glucose withdrawal [26]. Thus, mTORC1 positively controls ULK1 P-S555, but how? Shang et al. demonstrated that AMPK and ULK1 interact in complete media containing amino acids and glucose but dissociate partially upon the removal of amino acids [10,66] (Fig. 10B). Moreover, they found that blocking mTORC1-mediated phosphorylation of ULK1 S758 (mouse S757) using a non-phosphorylatable S758A mutant reduced the strength of the ULK1-AMPK interaction in complete media [10]. Integrating these results, we propose that mTORC1-mediated phosphorylation of ULK1 S757/S758 stabilizes the AMPK-ULK1 interaction, thus facilitating the ability of AMPK to

phosphorylate ULK1 S555 (and likely other sites), inhibit the ULK1 complex, and suppress autophagic initiation and progression (Fig. 10B).

Assays monitoring LC3b lipidation by western blot or LC3b or p62/SQSTM1 puncta formation by microscopy are prone to misinterpretation if not conducted rigorously, which may explain why the concept that AMPK promotes autophagy has continued over many years. For example, if the experimental design lacks an autophagic flux inhibitor, and if one interprets the above autophagy readouts through the established lens that AMPK promotes autophagy, then reduced levels of LC3-II or LC3 puncta upon inactivation of AMPK could be interpreted as "reduced" autophagy when in reality autophagy had been accelerated, leading to faster LC3b degradation in autolysosomes. We speculate that the absence of flux inhibitors in experimental designs may have led some groups to conclude that AMPK promotes autophagy [28,67]. It is important to note that the analysis of autophagy in mice using LC3b-II levels or LC3 puncta as the readout becomes even more challenging due to the inability to easily inhibit autophagic flux *in vivo*.

While this manuscript was in preparation, Park et al. reported findings overlapping with ours regarding the relationship between AMPK and autophagy [68]. By studying MEFs and HCT116 cells, they found that the activation of AMPK (using A769662, glucose withdrawal, or mitochondrial poisons) suppressed the ULK1-dependent phosphorylation of ATG14 and Beclin-1, the lipidation of LC3b, and the induction of LC3b and WIPI2 puncta induced by amino acid withdrawal [68]. Thus, they demonstrated that activation of AMPK suppresses ULK1 signaling, autophagic initiation, and autophagic progression during amino acid deprivation. Similarly, by studying MEFs and C2C12 cells, we found that the activation of AMPK (using compound 991, glucose withdrawal, or AICAR) suppressed ULK1-dependent phosphorylation of ATG16L1, the lipidation of LC3b, and the induction of LC3b and p62/SQSTM1 puncta. Like us and other groups [34,35], Park et al. observed that amino acid withdrawal or Torin1 treatment reduced AMPK-dependent ULK1 S555 phosphorylation [68]. Like Shang et al. [10], they demonstrated that amino acid withdrawal or Torin1 treatment destabilized the AMPK-ULK1 complex due to reduced mTORC1-mediated phosphorylation of ULK1 S757. Park et al. also demonstrated that AMPK-mediated phosphorylation of ULK1 S556 and T660 stabilizes the AMPK-ULK1 complex and inhibits ULK1-mediated phosphorylation of Beclin-1 and ATG14, likely by suppressing the kinase activity of the ULK1 complex [68]. We and Park et al. confirmed the findings of Nwadike et al., who showed that glucose deprivation not only fails to induce autophagy but suppresses autophagy induced by amino acid withdrawal [34,68]. We and Park et al. went further to demonstrate that the ability of glucose withdrawal to suppress autophagy induced by amino acid withdrawal requires AMPK. In summary, we and Park et al. agree that the activation of AMPK suppresses rather than promotes the induction of autophagy induced by amino acid withdrawal [68]. Moreover, together with Nwadike et al., we agree that glucose withdrawal not only fails to induce autophagy but suppresses autophagy in the context of amino acid deprivation [34,68].

Our results differ from the study by Park et al. in one respect, however. Park at al. found that the accumulation of LC3b-II was impaired in AMPKα DKO MEFs relative to wild type MEFs subjected to amino acid withdrawal (2 hr) in the presence of BafA1 [68]. In addition, they found that the kinase activity of the Vps34 complex, as measured by an *in vitro* assay, was lower in AMPKα DKO MEFs relative to wild type MEFs. They therefore concluded that AMPK plays dual roles in control of autophagy during amino acid deprivation: The activation of AMPK suppresses autophagy while its presence supports optimal autophagy. This latter idea aligns with the ability of AMPK to promote lysosomal biogenesis [69-72]. In contrast, we found that LC3b-II accumulated to a similar extent in wild type and AMPKα DKO MEFs deprived of amino acids (2 hr) and treated with BafA1 (see Fig. 2C, 2D; S2A-S2E). Note that we studied the same established wild type vs AMPKα DKO MEFs as Park et al. In addition, we found that the accumulation of LC3b-II remained intact in other AMPKα DKO cell lines (e.g., C2C12; HeLa; HEK293; U2OS) (see Fig. 2E, 2F and Fig. S2). When we generated a new line of control vs. AMPKα DKO MEFs using CRISPR/Cas9, we again found that the accumulation of LC3b-II in the presence of BafA1 remained unimpaired in AMPKα DKO MEFs relative to control MEFs deprived of amino acids (see Fig. S2A).

Moreover, when we normalized LC3b-II to LC3b-I, we found that AMPKα DKO MEFs and AMPKα DKD C2C12 cells converted LC3-I to LC3b-II faster than control cells in both the basal and amino acid-deprived states (see Fig. 2C-2F). The reason for the discrepancy between our results and those of Park et al. regarding the accumulation of LC3b-II in AMPKα double knockout MEFs remains unclear. Interestingly, Park et al. found that AMPKα DKO MEFs and HCT116 cells displayed elevated ULK1-dependent phosphorylation of ATG14 S29 relative to control cells during amino acid withdrawal [68]. These data align with ours, in which we found elevated ULK1-dependent phosphorylation of ATG16L1 S278 in AMPKα DKO MEFs and in AMPKα DKD C2C12 cells relative to control cells in the absence of amino acids (see Fig. 2C-2F).

Our work also reveals an unexpected relationship between AMPK and its control of mTORC1 signaling. During nutrient stress caused by prolonged amino acid deprivation, AMPK supports mTORC1 signaling, not by inducing autophagy, but by a new mechanism (Fig. 10A; 10C). Our work therefore challenges the idea that AMPK inhibits mTORC1 signaling in all cellular contexts. We speculate that during amino acid deprivation, AMPK-mediated support of mTORC1 signaling maintains essential metabolic processes necessary for cell survival (Fig. 10C). During severe energetic stress, however, AMPK inhibits mTORC1 to attenuate ATP-consuming anabolic metabolism to balance energy supply and demand, which also enhances cell survival. We hypothesize further that AMPK-mediated support of mTORC1 signaling during amino acid deprivation may represent a third mechanism by which AMPK limits autophagy. Thus, AMPK can respond to cell stress and affect mTORC1 signaling in different ways: During energetic stress (a rise in the AMP to ATP ratio) or mild glucose deprivation, AMPK reduces mTORC1 signaling [17-19,24], but during amino acid deprivation, AMPK supports mTORC1 signaling, thus preventing it from falling too low (this study). Both regulatory modes align with the conserved role of AMPK in sensing and responding to cell stress. How can AMPK inhibit mTORC1 during energetic stress or mild glucose deprivation yet support mTORC1 signaling during amino acid deprivation? Since AMPK can assemble into 12 potential isoforms due to its heterotrimeric nature and subunit diversity, we hypothesize that distinct isoforms of AMPK may control mTORC1 activity and function in different ways and in different contexts. Future work will be required to decipher the molecular mechanisms and AMPK isoforms underlying support of mTORC1 signaling in amino acid-deprived contexts.

In summary, our results demonstrate that the presence of AMPK and its acute activation each limit autophagy in the basal state and when induced by amino acid deprivation. Moreover, AMPK supports mTORC1 signaling during prolonged amino acid deprivation, not by inducing autophagy but by a new albeit unknown mechanism. Our findings therefore challenge the prevailing view that AMPK promotes autophagy and that AMPK always inhibits mTORC1, thus forcing a reexamination of the role of AMPK, mTOR, and autophagy in health and disease. Rather than inducing autophagy to generate metabolic building blocks that fuel energy production, we hypothesize that AMPK supports essential metabolic processes during nutrient stress (i.e., amino acid deprivation) but not energetic stress by supporting mTORC1 signaling.

Materials and Methods

Materials

General chemicals were from Thermo Fisher Scientific or Millipore Sigma. NP40 and Brij35 detergents were from Pierce. cOmplete Protease Inhibitor Cocktail tablets (EDTA-free) (11836170001) and Immobilon-polyvinylidene difluoride (PVDF) membrane (0.45 μM) (88518) were from Thermo Scientific. PhosSTOP phosphatase inhibitor cocktail tablets were from Roche (04906845001). Reagents for enhanced chemiluminescence (ECL) were from either Alkali Scientific (Bright Star XR92), Advansta (Western Bright Sirius HRP substrate), or Bio-Rad (1705061). Every Blot Blocking Buffer (12010020) and 4x Laemmli Sample Buffer (1610747) were from Bio-Rad. Torin1 was a gift from Dr. David Sabatini, Rapamycin was from Calbiochem (553210), compound 991 (ex229) was from Selleck (S8654), BAY-3827

was from Selleck (S9833), and Bafilomycin A1 was from Cayman (11038). LysoTracker was from Invitrogen (L7528). ReadyProbe cell viability reagents were from Thermo Fisher Scientific (R37609).

Antibodies

The following antibodies for western blots were from Cell Signaling Technology: LC3b (2775); P-AMPKα-T172 (4188); pan AMPKα1/α2 (2532); P-ULK1-S555 (5869); P-ULK1-S757 (23988); ULK1 (8054); p62/SQSTM1 (5114); P-S6K1-T389 (9234); cleaved caspase 3 (9664); cleaved PARP (9544); α-tubulin (2144); ATG5 (12994); P-Akt-S473 (4060); Akt (9272); and mTOR (2972). Antibodies for western blots also included the following: P-ATG16L1-S278 (Abcam, ab195242); ATG16L1 (Abcam, ab187671); S6K1 (amino acids 485-502; rat 70 kDa isoform) (custom-made, as described [73]. Donkey anti-rabbit-HRP (Jackson ImmunoResearch, 711-095-152) was used for detection of ECL-based western blot signals, we used. For confocal immunofluorescence microscopy, the following antibodies from Jackson ImmunoResearch were used: alexa 488-conjugated anti-rabbit-HRP (711545152) and alexa 594 conjugated anti-rat-HRP (112585167).

Generation of AMPKα1/α2 CRISPR DKO cells

We used CRISPR/Cas9-mediated genome editing technology [74] to knockout AMPKα1 (*PRKAA1)* and AMPKα2 (*PRKAA2)* from HeLa cells, C2C12 cells, HEK293 cells, and MEFs. Four mouse-specific gRNAs in total were used for targeting *PRKAA1* and *PRKAA2* in MEFs and C2C12 cells, two gRNAs for AMPKα1 and AMPKα2 each. These sequences were as described [75]: *PRKAA1* (A) GGCTGTCGCCATCTTTCTCC; (B) GAAGATCGGCCACTACATTC; *PRKAA2* (A) TCAGCCATCTTCGGCGCGCG; (B) GAAGATCGGACACTACGTGC. Two human-specific gRNAs in total were used for targeting *PRKAA1* and *PRKAA2* in HeLa and HEK293 cells, one gRNA for AMPKα1 and AMPKα2 each. These sequences were as described [69]: *PRKAA1* GTTATTGTCACAGGCATATGG; *PRKAA2* GACAGGCATATGGTTGTCCAT. These sequences are also listed in Supplementary Table 1. gRNAs were sub-cloned into vector pSpCas9(BB)-2A-Puro (PX459) (Addgene, 48139, deposited by the F. Zhang lab), and gRNA plasmids for targeting *PRKAA1* and *PRKAA2* were co-transfected into cells with TransIT-LT1 (Mirus, MIR 2305) according to the manufacturer's instructions. PX459 lacking a guide RNA was used to generate "control" cells. Cells transfected with PX459 plasmids were selected with puromycin for 72 hr, and drug-resistant colonies (or pools of colonies, indicated in the figure) were isolated and screened for AMPKα1/α2 double knockout by western blotting. The following puromycin concentrations were used for drug selection: HeLa [2 μg/mL]; C2C12 [4 μg/mL]; HEK293 [2 μg/mL]; MEFs [8 μg/mL]

Cell lines, cell culture, and cell treatments

Cell lines (MEFs; C2C12; HeLa; HEK293; U2OS) were cultured in DMEM containing high glucose [4.5 g/liter], glutamine [584 mg/liter] and sodium pyruvate [110 mg/liter] (Life Technologies/ Thermo Fisher, 11995-065) supplemented with 10% fetal bovine serum (FBS) (Life Technologies/ Thermo Fisher, 10347-028) and incubated at 37°C in a humidified atmosphere with 10% CO_2. The wild type and AMPKα1/α2 DKO MEFs, originally isolated from transgenic mice by Dr. B. Viollet (Inserme, Paris, France) [55] were shared by Dr. R. Shaw (Salk Institute, San Diego, CA). The WT and AMPKα1/α2 DKO U2OS cells were generated and shared by Dr. Reuben Shaw [75]. The wild type and ATG5 KO MEFs were shared by Dr. N. Mizushima (Tokyo Medical University, Tokyo, Japan) [76].

To study the effects of amino acid deprivation, we first fed cells at ~80% confluency with complete DMEM (containing FBS [10%], amino acids, and glucose) for 1 hr. We next washed cells with PBS containing Mg^{2+} and Ca^{2+} and refed them with precisely matched amino acid-replete DMEM (i.e., complete media) or amino-acid free DMEM containing dialyzed FBS [10%] and glucose [4.5 g/L] for various periods of time (0.5-16 hr) depending on the experiment. We prepared matched amino acid replete and amino acid-free media in the following way: Amino acid-free DMEM (US Biologicals, D9800-13) containing 10%

dialyzed FBS (Life Technologies, A33820-01) served as our amino acid deprivation media and as our base media for making complete media. To make complete media, we added a 50X RPMI 1640 amino acid solution (Sigma, R7131) supplemented with fresh glutamine ([300 mg/L] final) (Sigma, G8540) to the amino acid-free base media at 1x final amino acids. Importantly, prior to adding the 50x amino acid-glutamine solution to the amino acid-free DMEM, we adjusted the pH of this solution to 7.4, as the pH of the 50X RPMI amino acid solution is ~10. Note that it was critical to adjust the pH of the amino acid solution, as the addition of an alkaline solution to cultured cells activates AMPK, mTORC1, and mTORC2 due to a rise in intracellular pH [77,78]. To suppress autophagic proteolysis, cells were treated without or with BafA1 [1 μM] for the period of amino acid withdrawal or Torin1 treatment (i.e., 1, 2, or 4 hr), depending on the experiment. To stimulate cells with amino acids, the RPMI amino acid solution with L-glutamine (adjusted to pH 7.4) was added to cells in amino acid-free media at a 1x final concentration (diluted from a 50X stock). For glucose deprivation experiments, DMEM containing dFBS [10%] but lacking amino acids and glucose (US Biologicals, D9800-28) was reconstituted with the amino acid [1x] solution containing L-glutamine, D-glucose [4.5 g/L] (Sigma, G8270), or both before each experiment.

Cell lysis and immunoblotting

Cells were washed twice with ice-cold PBS, lysed in ice-cold buffer containing NP-40 [0.5%] and Brij35 [0.1%], and incubated on ice (15 min). Lysates were clarified by spinning at 16,100 x g for 5 min at 4°C, and the post-nuclear supernatants were collected. Bradford assay was used to normalize protein levels for immunoblot analyses. Samples were resolved on SDS-PAGE gels and transferred to PVDF membranes using the Bio-Rad Trans-Blot Turbo Transfer System according to the manufacturer's instructions. Immunoblotting was performed by blocking PVDF membranes in Tris-buffered saline (TBS) pH 7.5 with 0.1% Tween-20 (TBST) containing 3% non-fat dry milk and incubating the membranes in TBST containing 2% bovine serum albumin (BSA) containing primary antibodies or secondary HRP-conjugated antibodies. P-ATG16L1-S278 antibody was diluted at 1:4000 in EveryBlot blocking buffer (Bio-Rad, 12010020) and incubated overnight. Western blots were developed by enhanced chemiluminescence (ECL) and detected digitally with a UVP ChemStudio Imaging System from Analytik Jena equipped with VisionWorks 9.2 software.

RNA interference

AMPKα1 and α2 knockdown experiments in C2C12 cells were performed using scrambled control (Santa Cruz Biotechnology, sc-37007) or AMPKα1/α2-specific siRNAs (Santa Cruz Biotechnology, sc-45313) [10 nM]. C2C12 cells on 6-well plates were transiently transfected with RNAiMAX (Invitrogen, 13778-150) according to the manufacturer's directions in two stages to prevent over-confluency at the time of cellular treatment and lysis. Cells were first transfected at ~30-40% confluency and transfected again 24 hr later at 10-20% confluency. Cells were treated and lysed 72 hr after the first transfection at ~80-95% confluency.

Confocal immunofluorescence microscopy

Cells were seeded on glass coverslips in 6-well plates. Following various treatments, cells were washed with cold PBS^+ and fixed with 3.7% formaldehyde for 10 min. Cells were washed twice with PBS^+, permeabilized in 0.2% TX-100 for 5 min, washed twice with PBS^+, and blocked in 0.2% fish skin gelatin (FSG) for 1 hr. Coverslips were inverted on primary antibodies (1:100) (rabbit anti-P-ATG16L1-S278, Abcam, ab195242; rabbit anti-p62, CST, 2321) diluted in PBS^+ containing 0.2% FSG and incubated overnight. Cells were washed 3 times with PBS^+, and coverslips were inverted on Alexa 594-conjugated anti-rabbit antibody (1:500) (Jackson, 711585152) or Alexa 488-conjugated anti-rabbit antibody (1:500) (Jackson, 711545152) diluted in PBS^+/ 0.2% FSG, incubated for 1 hr, and washed 3 times with PBS^+. Coverslips for LC3b were fixed with ice-cold methanol at -20°C for 15 min, washed 3 times with PBS^+, and blocked in PBS^+ with 0.2% FSG and 0.3% TX-100 for 1 hr. Coverslips were incubated overnight with

250 μL primary antibody (1:100) (Alexa 488-conjugated mouse anti-LC3b, CST, 98557) diluted in PBS^+ containing 0.2% FSG and 0.3% TX-100 and washed 3 times with PBS^+. LysoTracker experiments were performed by adding LysoTracker Red DND-99 (Invitrogen, L7528) (50 nM) to the media for the last 30 minutes of treatment. Coverslips were mounted on slides using Prolong Gold with DAPI (CST, 8961). Images were captured using a 40x objective lens on a Zeiss LSM800 Confocal Laser Scanning Microscope. ImageJ/ Fiji (National Institutes of Health) was used to quantitate the numbers of puncta/ cell for LC3b, P-ATG16L1-S278, and p62 staining and to quantitate LysoTracker staining intensity over a field of multiple cells.

Transmission electron microscopy (TEM)

Cells were seeded on MatTek dishes. Following various treatments, cells were fixed overnight at 4°C in 2.5% glutaraldehyde in 0.1 M cacodylate buffer (pH 7.2) and washed with 0.1 M cacodylate buffer (pH 7.2) three times for 5 minutes each at room temperature. Cells were post-fixed in 1% $K_4Fe(CN)_6$ and 1% OsO_4 in 0.1 M cacodylate buffer (pH 7.2) for 15 minutes at 4°C. Samples were washed three times for 3 minutes each with 0.1 M cacodylate buffer (pH 7.2) at room temperature, and then samples were washed with 0.1 M sodium acetate buffer (pH 5.2) three times for two minutes each at room temperature. Samples were en bloc stained with 2% uranyl acetate (in 0.1 M sodium acetate buffer (pH 5.2) for 15 minutes at room temperature. Samples were washed three times for 1 minute each with deionized water at room temperature. The cells were stained with Walton's lead aspartate for 15 minutes at 60°C. Samples were washed three times for 3 minutes each with 0.1 M sodium acetate buffer (pH 5.2) at room temperature and three times with water for 3 minutes. The cells were dehydrated with a series of ethanol concentrations (10, 30, 50, 70, 80, 90, and 95%), 5 minutes each at 4°C, and finally, dehydrated twice with 100% ethanol for 5 minutes at room temperature. The cells were infiltrated with a 2:1 ratio of 100% ethanol to Araldite 502-Embed 812 for 30 minutes and 10 hr in a 1:2 ratio of 100% ethanol to Araldite 502-Embed 812 at room temperature. Finally, cells were infiltrated overnight with 100% Araldite 502/Embed 812. Cells were polymerized for 24 hr at 70°C and sectioned with a Leica UC7 ultramicrotome at 70 nm. The samples were imaged on a Jeol-1400 Plus Transmission Electron Microscope.

Cell viability assay

Cells were seeded on 35 mm polylysine-coated glass bottom plates and amino acid-deprived for 16 hr. Cell viability was assessed by adding ReadyProbe reagents (Thermo Fisher Scientific, R37609) for the last 15 min of incubation according to the manufacturers' directions. NucBlue Live reagent (Hoechst 33342) stains the nuclei of all cells, whereas NucGreen Dead stains the nuclei of cells with compromised plasma membranes (i.e., dead cells). Images were collected on an inverted epifluorescence microscope (Nikon TE2000E) equipped with a Photometrics CoolSnap HQ camera and analyzed using ImageJ/ Fiji (National Institutes of Health).

Image editing

Adobe Photoshop was used to prepare digital western blot images for presentation, using only the levels, brightness, and contrast controllers equivalently over the entire image.

Statistical analysis

Results are presented as mean ± standard deviation (SD). Data were analyzed by one-way or two-way ANOVA followed by Sidak's multiple comparison post hoc tests or by unpaired Student's t-tests, as indicated in the figure legends. Values of $p < 0.05$ were considered significant. $^*p<0.05$; $^{**}p<0.01$; $^{***}p<0.001$; $^{****}p<0.00001$.

Acknowledgments

We thank Dr. R. Shaw for sharing the wild type and AMPK DKO MEFs, originally generated by Dr. B. Viollet. We thank Dr. JH Lee for sharing the wild type and ATG5 KO MEFs, originally generated by N. Mizushima. We thank Dr. D. Sabatini for sharing Torin1.

Disclosure statement. We attest that we have no competing interests. Funders or other external entities played no role in the experimental design, execution, or analysis of this work.

Funding. This work was supported by grants to DCF from the NIH (R01-GM137577) and by the Michigan Diabetes Research Center (MDRC) (NIH-P30-DK020572).

References

[1] Yu L, Chen Y, Tooze SA. Autophagy pathway: Cellular and molecular mechanisms. Autophagy. 2018;14(2):207-215.
[2] King KE, Losier TT, Russell RC. Regulation of Autophagy Enzymes by Nutrient Signaling. Trends Biochem Sci. 2021 Aug;46(8):687-700.
[3] Lahiri V, Hawkins WD, Klionsky DJ. Watch What You (Self-) Eat: Autophagic Mechanisms that Modulate Metabolism. Cell Metab. 2019 Apr 2;29(4):803-826.
[4] Klionsky DJ, Petroni G, Amaravadi RK, et al. Autophagy in major human diseases. EMBO J. 2021 Oct 1;40(19):e108863.
[5] Ben-Sahra I, Manning BD. mTORC1 signaling and the metabolic control of cell growth. Curr Opin Cell Biol. 2017 Apr;45:72-82.
[6] Gonzalez A, Hall MN. Nutrient sensing and TOR signaling in yeast and mammals. EMBO J. 2017 Feb 15;36(4):397-408.
[7] Kim J, Guan KL. mTOR as a central hub of nutrient signalling and cell growth. Nat Cell Biol. 2019 Jan;21(1):63-71.
[8] Battaglioni S, Benjamin D, Walchli M, et al. mTOR substrate phosphorylation in growth control. Cell. 2022 May 26;185(11):1814-1836.
[9] Kim J, Guan KL. Regulation of the autophagy initiating kinase ULK1 by nutrients: roles of mTORC1 and AMPK. Cell cycle. 2011 May 1;10(9):1337-8.
[10] Shang L, Chen S, Du F, et al. Nutrient starvation elicits an acute autophagic response mediated by Ulk1 dephosphorylation and its subsequent dissociation from AMPK. Proc Natl Acad Sci U S A. 2011 Mar 22;108(12):4788-93.
[11] Carroll B, Dunlop EA. The lysosome: a crucial hub for AMPK and mTORC1 signalling. Biochem J. 2017 Apr 13;474(9):1453-1466.
[12] Rabanal-Ruiz Y, Otten EG, Korolchuk VI. mTORC1 as the main gateway to autophagy. Essays Biochem. 2017 Dec 12;61(6):565-584.
[13] Dossou AS, Basu A. The Emerging Roles of mTORC1 in Macromanaging Autophagy. Cancers (Basel). 2019 Sep 24;11(10).
[14] Zachari M, Ganley IG. The mammalian ULK1 complex and autophagy initiation. Essays Biochem. 2017 Dec 12;61(6):585-596.
[15] Klionsky DJ, Abdel-Aziz AK, Abdelfatah S, et al. Guidelines for the use and interpretation of assays for monitoring autophagy (4th edition)(1). Autophagy. 2021 Jan;17(1):1-382.
[16] Mizushima N, Yoshimori T. How to interpret LC3 immunoblotting. Autophagy. 2007 Nov-Dec;3(6):542-5.
[17] Inoki K, Zhu T, Guan KL. TSC2 mediates cellular energy response to control cell growth and survival. Cell. 2003 Nov 26;115(5):577-90.
[18] Gwinn DM, Shackelford DB, Egan DF, et al. AMPK phosphorylation of raptor mediates a metabolic checkpoint. Mol Cell. 2008 Apr 25;30(2):214-26.

[19] Zhang CS, Jiang B, Li M, et al. The lysosomal v-ATPase-Ragulator complex is a common activator for AMPK and mTORC1, acting as a switch between catabolism and anabolism. Cell Metab. 2014 Sep 2;20(3):526-40.
[20] Herzig S, Shaw RJ. AMPK: guardian of metabolism and mitochondrial homeostasis. Nat Rev Mol Cell Biol. 2018 Feb;19(2):121-135.
[21] Steinberg GR, Carling D. AMP-activated protein kinase: the current landscape for drug development. Nat Rev Drug Discov. 2019 Jul;18(7):527-551.
[22] Gonzalez A, Hall MN, Lin SC, et al. AMPK and TOR: The Yin and Yang of Cellular Nutrient Sensing and Growth Control. Cell Metab. 2020 Mar 3;31(3):472-492.
[23] Steinberg GR, Hardie DG. New insights into activation and function of the AMPK. Nat Rev Mol Cell Biol. 2023 Apr;24(4):255-272.
[24] Zhang CS, Hawley SA, Zong Y, et al. Fructose-1,6-bisphosphate and aldolase mediate glucose sensing by AMPK. Nature. 2017 Aug 3;548(7665):112-116.
[25] Kim J, Kundu M, Viollet B, et al. AMPK and mTOR regulate autophagy through direct phosphorylation of Ulk1. Nat Cell Biol. 2011 Feb;13(2):132-41.
[26] Egan DF, Shackelford DB, Mihaylova MM, et al. Phosphorylation of ULK1 (hATG1) by AMP-activated protein kinase connects energy sensing to mitophagy. Science. 2011 Jan 28;331(6016):456-61.
[27] Kim J, Kim YC, Fang C, et al. Differential regulation of distinct Vps34 complexes by AMPK in nutrient stress and autophagy. Cell. 2013 Jan 17;152(1-2):290-303.
[28] Zhang D, Wang W, Sun X, et al. AMPK regulates autophagy by phosphorylating BECN1 at threonine 388. Autophagy. 2016 Sep;12(9):1447-59.
[29] Egan D, Kim J, Shaw RJ, et al. The autophagy initiating kinase ULK1 is regulated via opposing phosphorylation by AMPK and mTOR. Autophagy. 2011 Jun;7(6):643-4.
[30] Mao K, Klionsky DJ. AMPK activates autophagy by phosphorylating ULK1. Circ Res. 2011 Apr 1;108(7):787-8.
[31] Wang S, Li H, Yuan M, et al. Role of AMPK in autophagy. Front Physiol. 2022;13:1015500.
[32] Lang MJ, Martinez-Marquez JY, Prosser DC, et al. Glucose starvation inhibits autophagy via vacuolar hydrolysis and induces plasma membrane internalization by down-regulating recycling. J Biol Chem. 2014 Jun 13;289(24):16736-47.
[33] Ramirez-Peinado S, Leon-Annicchiarico CL, Galindo-Moreno J, et al. Glucose-starved cells do not engage in prosurvival autophagy. J Biol Chem. 2013 Oct 18;288(42):30387-30398.
[34] Nwadike C, Williamson LE, Gallagher LE, et al. AMPK Inhibits ULK1-Dependent Autophagosome Formation and Lysosomal Acidification via Distinct Mechanisms. Mol Cell Biol. 2018 May 15;38(10).
[35] Artal-Martinez de Narvajas A, Gomez TS, Zhang JS, et al. Epigenetic regulation of autophagy by the methyltransferase G9a. Mol Cell Biol. 2013 Oct;33(20):3983-93.
[36] Jeon SM, Hay N. The dark face of AMPK as an essential tumor promoter. Cell Logist. 2012 Oct 1;2(4):197-202.
[37] Svensson RU, Shaw RJ. Cancer metabolism: Tumour friend or foe. Nature. 2012 May 31;485(7400):590-1.
[38] Hardie DG. The LKB1-AMPK pathway-friend or foe in cancer? Cancer cell. 2013 Feb 11;23(2):131-2.
[39] Vara-Ciruelos D, Russell FM, Hardie DG. The strange case of AMPK and cancer: Dr Jekyll or Mr Hyde? (dagger). Open Biol. 2019 Jul 26;9(7):190099.
[40] Russell FM, Hardie DG. AMP-Activated Protein Kinase: Do We Need Activators or Inhibitors to Treat or Prevent Cancer? Int J Mol Sci. 2020 Dec 27;22(1).
[41] Sadria M, Seo D, Layton AT. The mixed blessing of AMPK signaling in Cancer treatments. BMC Cancer. 2022 Jan 25;22(1):105.

[42] Sancak Y, Peterson TR, Shaul YD, et al. The Rag GTPases bind raptor and mediate amino acid signaling to mTORC1. Science. 2008 Jun 13;320(5882):1496-501.
[43] Kim E, Goraksha-Hicks P, Li L, et al. Regulation of TORC1 by Rag GTPases in nutrient response. Nat Cell Biol. 2008 Aug;10(8):935-45.
[44] Sancak Y, Bar-Peled L, Zoncu R, et al. Ragulator-Rag complex targets mTORC1 to the lysosomal surface and is necessary for its activation by amino acids. Cell. 2010 Apr 16;141(2):290-303.
[45] Yu L, McPhee CK, Zheng L, et al. Termination of autophagy and reformation of lysosomes regulated by mTOR. Nature. 2010 Jun 17;465(7300):942-6.
[46] Yu X, Long YC. Autophagy modulates amino acid signaling network in myotubes: differential effects on mTORC1 pathway and the integrated stress response. FASEB J. 2015 Feb;29(2):394-407.
[47] Puertollano R. mTOR and lysosome regulation. F1000Prime Rep. 2014;6:52.
[48] Chen Y, Yu L. Recent progress in autophagic lysosome reformation. Traffic. 2017 Jun;18(6):358-361.
[49] Fu W, Hall MN. Regulation of mTORC2 Signaling. Genes (Basel). 2020 Sep 4;11(9).
[50] Szwed A, Kim E, Jacinto E. Regulation and metabolic functions of mTORC1 and mTORC2. Physiol Rev. 2021 Feb 18.
[51] Bar-Peled L, Schweitzer LD, Zoncu R, et al. Ragulator is a GEF for the rag GTPases that signal amino acid levels to mTORC1. Cell. 2012 Sep 14;150(6):1196-208.
[52] Kazyken D, Magnuson B, Bodur C, et al. AMPK directly activates mTORC2 to promote cell survival during acute energetic stress. Sci Signal. 2019 Jun 11;12(585).
[53] Shaw RJ, Kosmatka M, Bardeesy N, et al. The tumor suppressor LKB1 kinase directly activates AMP-activated kinase and regulates apoptosis in response to energy stress. Proc Natl Acad Sci U S A. 2004 Mar 9;101(10):3329-35.
[54] Tian W, Alsaadi R, Guo Z, et al. An antibody for analysis of autophagy induction. Nat Methods. 2020 Feb;17(2):232-239.
[55] Laderoute KR, Amin K, Calaoagan JM, et al. 5'-AMP-activated protein kinase (AMPK) is induced by low-oxygen and glucose deprivation conditions found in solid-tumor microenvironments. Mol Cell Biol. 2006 Jul;26(14):5336-47.
[56] Lemos C, Schulze VK, Baumgart SJ, et al. The potent AMPK inhibitor BAY-3827 shows strong efficacy in androgen-dependent prostate cancer models. Cell Oncol (Dordr). 2021 Jun;44(3):581-594.
[57] Kim PK, Hailey DW, Mullen RT, et al. Ubiquitin signals autophagic degradation of cytosolic proteins and peroxisomes. Proc Natl Acad Sci U S A. 2008 Dec 30;105(52):20567-74.
[58] Thoreen CC, Sabatini DM. Rapamycin inhibits mTORC1, but not completely. Autophagy. 2009 Jul;5(5):725-6.
[59] Zhao J, Zhai B, Gygi SP, et al. mTOR inhibition activates overall protein degradation by the ubiquitin proteasome system as well as by autophagy. Proc Natl Acad Sci U S A. 2015 Dec 29;112(52):15790-7.
[60] Williams T, Forsberg LJ, Viollet B, et al. Basal autophagy induction without AMP-activated protein kinase under low glucose conditions. Autophagy. 2009 Nov;5(8):1155-65.
[61] Samari HR, Seglen PO. Inhibition of hepatocytic autophagy by adenosine, aminoimidazole-4-carboxamide riboside, and N6-mercaptopurine riboside. Evidence for involvement of amp-activated protein kinase. J Biol Chem. 1998 Sep 11;273(37):23758-63.
[62] Plomp PJ, Wolvetang EJ, Groen AK, et al. Energy dependence of autophagic protein degradation in isolated rat hepatocytes. European journal of biochemistry / FEBS. 1987 Apr 1;164(1):197-203.
[63] Schellens JP, Vreeling-Sindelarova H, Plomp PJ, et al. Hepatic autophagy and intracellular ATP. A morphometric study. Exp Cell Res. 1988 Jul;177(1):103-8.

[64] Thomas HE, Zhang Y, Stefely JA, et al. Mitochondrial Complex I Activity Is Required for Maximal Autophagy. Cell reports. 2018 Aug 28;24(9):2404-2417 e8.
[65] Puente C, Hendrickson RC, Jiang X. Nutrient-regulated Phosphorylation of ATG13 Inhibits Starvation-induced Autophagy. J Biol Chem. 2016 Mar 11;291(11):6026-6035.
[66] Shang L, Wang X. AMPK and mTOR coordinate the regulation of Ulk1 and mammalian autophagy initiation. Autophagy. 2011 Aug;7(8):924-6.
[67] Lee JW, Park S, Takahashi Y, et al. The association of AMPK with ULK1 regulates autophagy. PLoS One. 2010 Nov 3;5(11):e15394.
[68] Park JM, Lee DH, Kim DH. Redefining the role of AMPK in autophagy and the energy stress response. Nature communications. 2023 May 24;14(1):2994.
[69] Young NP, Kamireddy A, Van Nostrand JL, et al. AMPK governs lineage specification through Tfeb-dependent regulation of lysosomes. Genes Dev. 2016 Mar 1;30(5):535-52.
[70] Paquette M, El-Houjeiri L, L CZ, et al. AMPK-dependent phosphorylation is required for transcriptional activation of TFEB and TFE3. Autophagy. 2021 Dec;17(12):3957-3975.
[71] Malik N, Ferreira BI, Hollstein PE, et al. Induction of lysosomal and mitochondrial biogenesis by AMPK phosphorylation of FNIP1. Science. 2023 Apr 21;380(6642):eabj5559.
[72] Freemantle JB, Hardie DG. AMPK promotes lysosomal and mitochondrial biogenesis via folliculin:FNIP1. Life Metab. 2023 Oct;2(5):load027.
[73] Acosta-Jaquez HA, Keller JA, Foster KG, et al. Site-specific mTOR phosphorylation promotes mTORC1-mediated signaling and cell growth. Mol Cell Biol. 2009 Aug;29(15):4308-24.
[74] Ran FA, Hsu PD, Wright J, et al. Genome engineering using the CRISPR-Cas9 system. Nat Protoc. 2013 Nov;8(11):2281-2308.
[75] Toyama EQ, Herzig S, Courchet J, et al. Metabolism. AMP-activated protein kinase mediates mitochondrial fission in response to energy stress. Science. 2016 Jan 15;351(6270):275-281.
[76] Kuma A, Hatano M, Matsui M, et al. The role of autophagy during the early neonatal starvation period. Nature. 2004 Dec 23;432(7020):1032-6.
[77] Kazyken D, Lentz SI, Fingar DC. Alkaline intracellular pH (pHi) activates AMPK-mTORC2 signaling to promote cell survival during growth factor limitation. J Biol Chem. 2021 Oct;297(4):101100.
[78] Kazyken D, Lentz SI, Wadley M, et al. Alkaline intracellular pH (pHi) increases PI3K activity to promote mTORC1 and mTORC2 signaling and function during growth factor limitation. J Biol Chem. 2023 Sep;299(9):105097.

Supplemental Information. See Supplementary Materials for Figures S1-S5.

Figure legends

Figure 1. AMPKα1/α2 double knockout increases apoptotic cell death and impairs the reactivation of mTORC1 signaling during prolonged amino acid deprivation

(**A)** WT and AMPKα DKO MEFs, generated by Laderoute et al. [55], were fed with complete media (+) for 1 hr or amino acid-free media (-) for 0.5 – 16 hr. Attached and floating cells were collected. Whole cell lysates were immunoblotted as indicated.
(**B)** Control and AMPKα DKO HeLa cells were treated as in (A).
(**C)** MEFs were treated as in (A), except ReadyProbe cell viability reagents were added to the culture media. Green fluorescence marks dead cells, while blue (Dapi) fluorescence marks total cells.

(**D**) Percent (%) cell death is indicated by the ratio of green cells/ total blue cells. n = 100 cells per treatment from 1 representative experiment. Two-way ANOVA was performed followed by Sidak's multiple comparison post hoc tests; ****$p < 0.0001$; ns, not significant.
(**E**) WT and AMPKα DKO MEFs were fed with complete media (+) for 1 hr or amino acid-free media (-) for 0.5-6 hr.
(**F**) Control and AMPKα DKO HeLa cells were treated as in (E).
(**G**) WT MEFs were fed with complete media (+) for 1 hr or amino acid-free media (-) for 1, 2, or 4 hr in the absence or presence of BafA1 [1 μM]. LE: light exposure; DE: dark exposure.
(**H**) WT HeLa cells were treated as in (G).
(**I**) Model: In complete media containing amino acids and glucose, mTORC1 suppresses autophagy. Acute withdrawal of amino acids (or treatment with Torin1) inhibits mTORC1 rapidly, which initiates autophagy. Autophagic proteolysis generates free amino acids, which reactivate mTORC1 partially in an AMPK-dependent manner. In this study, we demonstrate that impaired induction of autophagy cannot explain the impaired reactivation of mTORC1 upon prolonged amino acid withdrawal in AMPKα DKO cells, because AMPK is not essential for the induction of autophagy by amino acid deprivation (red arrow with "X"). Moreover, our results indicate that AMPK suppresses autophagy (blue line). Thus, AMPK supports mTORC1 signaling during prolonged amino acid deprivation by an unknown mechanism (blue dotted arrow).

Figure 2. AMPKα1/α2 double knockout/down increases basal (i.e., constitutive) and amino acid withdrawal-induced autophagy

(**A**) WT and AMPKα DKO MEFs were fed with complete media (+) for 1 hr or amino acid-free media (-) for 1, 2, or 4 hr in the absence or presence of BafA1 [1 μM]. Whole cell lysates were immunoblotted as indicated. LE: light exposure; DE: dark exposure.
(**B**) C2C12 cells were transiently transfected with scrambled (Scr) or AMPKα1 and α2 siRNA and treated as in (A).
(**C**) WT and AMPKα DKO MEFs were fed with complete (+) or amino acid-free media (-) for 2 hr in the absence or presence of BafA1 [1 μM].
(**D**) Quantification of LC3b-II/ α-Tubulin, LC3b-II/ LC3b-I, and P-ATG16L1-S278/ ATG16L1 from (C). n = 3 independent experiments.
(**E**) C2C12 cells were transiently transfected with scrambled or AMPKα1/α2 siRNA and treated as in (C).
(**F**) Quantification of LC3b-II/ α-Tubulin, LC3b-II/ LC3b-I, and P-ATG16L1-S278/ ATG16L1 from (E). n= 4 independent experiments.
(**G)** WT and AMPKα DKO MEFs were treated as in (A) without BafA1.
(**H**) C2C12 cells were transiently transfected with siRNA as in (E) and treated as in (A) without BafA1.

Bars on graphs represent mean +/- SD (standard deviation). Two-way ANOVA was performed followed by Sidak's multiple comparison post hoc tests; *$p < 0.05$; **$p < 0.01$; ***$p < 0.001$; ****$p < 0.0001$; ns, not significant.

Figure 3. Autophagy induced by pharmacological mTORC1 inhibition occurs unimpaired in cells lacking AMPKα1/α2

(**A**) WT and AMPKα DKO MEFs were fed with complete media for 1 hr and then treated without (-) or with (+) Torin1 [100 nM] for 1-4 hr in the absence or presence of BafA1 [1 μM]. Whole cell lysates were immunoblotted as indicated. LE: light exposure; DE: dark exposure.
(**B**) C2C12 cells were transiently transfected with scrambled (Scr) or AMPKα1/α2 siRNA and treated as in (A).

(**C and D**) Quantification of LC3b-II/ α-Tubulin, LC3b-II/ LC3b-I, and P-ATG16L1-S278/ ATG16L1 from (A) and (B), respectively (2 hr time point). Data represented as mean ± S.D. n = 4 independent experiments. Two-way ANOVA was performed followed by Sidak's multiple comparison post hoc tests; *$p < 0.05$; **$p < 0.01$; ***$p < 0.001$; ****$p < 0.0001$; ns, not significant.
(**E**) WT and AMPKα DKO MEFs were treated as in (A) without BafA1.
(**F**) C2C12 cells were transiently transfected with siRNA as in (B) and treated as in (A) without BafA1.

Figure 4. Induction of LC3, P-ATG16L1-S278, and p62 puncta by amino acid deprivation occurs unimpaired in cells lacking AMPKα1/α2, with evidence of increased autophagy in the absence of AMPK

(**A**) WT and AMPKα DKO MEFs were fed with complete (+) or amino acid-free media (-) for 2 hr in the presence of BafA1 [1 μM]. Cells were fixed and stained for endogenous LC3b. Scale bar: 10 μm.
(**B**) Quantification of LC3b puncta number from (A). n = 30-40 cells from one experiment, representative of 4 independent experiments.
(**C**) C2C12 cells were transiently transfected with scrambled (Scr) or AMPKα1 and α2 siRNA and treated as in (A). Scale bar: 10 μm.
(**D**) Quantification of LC3b puncta number from (C). n = 60-70 cells from two of four independent experiments. Below: Level of siRNA-mediated AMPKα knockdown in (C).
(**E**) WT and AMPKα1/α2 DKO MEFs were fed with complete (+) or amino acid-free media (-) for 2 hr in the absence of BafA1. Cells were fixed and stained for endogenous P-ATG16L1-S278. Scale bar: 5 μm.
(**F**) Quantification of P-ATG16L1-S278 puncta number from (E). n = 40 cells from two independent experiments.
(**G**) C2C12 cells were transiently transfected with siRNA as in (C), fixed, and stained for endogenous P-ATG16L1-S278. Scale bar: 5 μm.
(**H**) Quantification of ATG16L1 P-S278 puncta number from (G). n = 30-40 cells from one of two independent experiments. Below: Level of siRNA-mediated AMPKα knockdown in (G).
(**I**) WT and AMPKα DKO MEFs were fed with complete (+) or amino acid-free media (-) for 2 hr in the presence of BafA1 [1 μM]. Cells were fixed and stained for endogenous p62. Scale bar: 10 μm.
(**J**) Quantification of p62 puncta from (I). n = 60-70 cells from 2 independent experiments.

Bars on graphs represent mean +/- SD (standard deviation). Two-way ANOVA was performed followed by Sidak's multiple comparison post hoc tests; ***$p < 0.001$; ****$p < 0.0001$; ns, not significant.

Figure 5. Formation of autophagosomes upon prolonged amino acid deprivation occurs unimpaired in cells lacking AMPKα1/α2

A. WT and AMPKα DKO MEFs were fed with complete (+ AA) or amino acid-free media (- AA) for 2 hr in the presence of BafA1 [1 μM]. Cells were fixed, and the formation of autophagosomal- and autolysosomal-like structures were monitored by transmission electron microscope (TEM). White arrowheads denote typical structures counted and quantified in B. An enlarged view of the dotted box from the middle panel (-AA) is shown in the panels on the right (Enlarged view). Scale bar: 1 μm.
B. Quantification of the numbers of autophagosomal- and autolysosomal-like structures in (A). n = 40 fields of individual cells from one experiment.
C. C2C12 cells were transiently transfected with scrambled (Scr) or AMPKα1/α2 siRNA and treated and analyzed as in (A). Scale bar: 1 μm.
D. Quantification of the numbers of autophagosomal- and autolysosomal-like structures from (C). n = 40 fields of individual cells from one experiment. Right panel: Level of siRNA-mediated AMPKα knockdown in (C).

Bars on graphs represent mean +/- SD (standard deviation). Two-way ANOVA was performed followed by Sidak's multiple comparison post hoc tests; *$p < 0.05$; ****$p < 0.0001$; ns, not significant.

Figure 6. Activation of AMPK suppresses ULK1 signaling induced by amino acid deprivation while AMPKα1/α2 double knockout/down increases lysosomal acidification

(**A**) WT and AMPKα DKO MEFs were pre-treated without or with compound 991 [10 μM] (30 min) and refed with complete (+) or amino acid-free (-) media for 2 hr in the absence or presence of 991 and absence of BafA1. Whole cell lysates were immunoblotted as indicated.
(**B**) Quantification of P-ATG16L1-S278/ATG16L1 in complete media (left panel) and amino acid-free media (right panel) from (A). n = 4 independent experiments.
(**C**) C2C12 cells were transiently transfected with scrambled (Scr) or AMPKα1/α2 siRNA and treated as in (A).
(**D**) Quantification of P-ATG16L1-S278/ATG16L1 in complete media (left panel) and amino acid-free media (right panel) from (C). n = 3 independent experiments.
(**E**) WT and AMPKα DKO MEFs were pre-treated without or with MRT68921 [10 μM] (30 min) and re-fed with complete (+) or amino acid-free (-) media for 2 hr in the absence or presence of MRT68921 and absence of BafA1.
(**F**) Quantification of P-ATG16L1-S278/ATG16L1 from (E). n = 4 independent experiments.
(**G**) WT and AMPKα DKO MEFs were fed with complete (+) or amino acid-free (-) media in the presence or absence of glucose (Glc) for 2 hr and absence of BafA1.
(**H**) Quantification of P-ATG16L1-S278/ATG16L1 in complete media (left panel) and amino acid-free media (right panel) from (G). n = 5 independent experiments.
(**I**) C2C12 cells were transiently transfected with siRNA as in (C) and treated as in (G).
(**J**) Quantification of P-ATG16L1-S278/ATG16L1 in complete media (left panel) and amino acid-free media (right panel) from (I). n = 3 independent experiments.
(**K**) WT and AMPKα DKO MEFs were fed with complete (+) or amino acid-free (-) media for 2 hr in the absence of BafA1, treated with LysoTracker (30 min) and fixed. Scale bar: 10 μm.
(**L**) Quantification of LysoTracker intensity from (K). n = 10 fields of cells with 4-6 cells/field (~40-60 cells) from one experiment, representative of 2 independent experiments.
(**M**) WT and AMPKα DKO C2C12 cells (CRISPR clone #16) were fed with complete (+) or amino acid-free (-) media for 2 hr in the absence of BafA1, treated with LysoTracker (30 min), and fixed. Scale bar: 10 μm.
(**N**) Quantification of LysoTracker intensity from (M). n = 20 fields of cells with 15-20 cells/field (~300-400 cells) from one experiment, representative of 2 independent experiments.

Bars on graphs represent mean +/- SD (standard deviation). Two-way ANOVA was performed followed by Sidak's multiple comparison post hoc tests; *$p < 0.05$; **$p < 0.01$; ***$p < 0.001$; ****$p < 0.0001$; ns, not significant.

Figure 7. Activation of AMPK suppresses autophagic progression induced by amino acid deprivation

(**A**) WT and AMPKα DKO MEFs were pre-treated without or with compound 991 [10 μM] (30 min) and fed with complete (+) or amino acid-free media (-) for 2 hr in the absence or presence of 991 and presence of BafA1 [1 μM]. Whole cell lysates were immunoblotted as indicated. LE: light exposure; DE: dark exposure.
(**B**) Quantification of LC3b-II/α-Tubulin (upper panel) and LC3b-II/LC3b-I (lower panel) from (A). n = 4 independent experiments.
(**C**) C2C12 cells were transiently transfected with scrambled (Scr) or AMPKα1/α2 siRNA and treated as in (A).

(**D**) Quantification of LC3b-II/α-Tubulin (upper panel) and LC3b-II/LC3b-I (lower panel) from (C). n = 4 independent experiments.
(**E**) WT MEFs were pre-treated without or with 991 [10 μM] (30 min) and fed with complete (+) or amino acid-free (-) media in the absence or presence of 991 and presence of BafA1 [1 μM] for 2 hr. Cells were fixed and stained for endogenous LC3b. Scale bar: 10 μm.
(**F**) Quantification of LC3b puncta number from (E). n = 40 cells from 2 independent experiments.
(**G**) WT C2C12 cells were treated as in (E). Scale bar: 10 μm.
(**H**) Quantification of LC3b puncta number from (G). n = 40 cells from 2 independent experiments.
(**I**) WT and AMPKα DKO MEFs were fed with complete (+) or amino acid-free (-) media for 2 hr in the presence or absence of glucose (Glc) and the presence of BafA1 [1 μM].
(**J**) Quantification of LC3b-II/α-Tubulin (upper panel) and LC3b-II/LC3b-I (lower panel) from (I). n = 4 independent experiments.
(**K**) C2C12 cells were transiently transfected with siRNA as in (C) and treated as in (A).
(**L**) Quantification of LC3b-II/α-Tubulin (upper panel) and LC3b-II/LC3b-I (lower panel) from (K). n = 4 independent experiments.

Bars on graphs represent mean +/- SD (standard deviation). Two-way ANOVA was performed followed by Sidak's multiple comparison post hoc tests; *$p < 0.05$; **$p < 0.01$; ***$p < 0.001$; ****$p < 0.0001$; ns, not significant.

Figure 8. Activation of AMPK suppresses autophagic initiation and progression induced by pharmacological mTORC1 inhibition

(**A**) WT MEFs were pre-treated first without or with rapamycin [20 nM] or Torin1 [100 nM] (30 min), then pre-treated without or with 991 [10 μM] (30 min), and then fed with complete (+) or amino acid-free (-) media lacking or containing the drugs above for 2 hr in the presence of BafA1 [1 μM]. Whole cell lysates were immunoblotted as indicated (total treatment time, 3 hr). LE, light exposure; DE, dark exposure.
(**B**) Quantification of LC3b-II/α-Tubulin (left panels) and P-ATG16L1-S278/ATG16L1 (right panels) from (A). Upper panels: Torin1-treated cells; lower panels: rapamycin-treated cells. n = 4 independent experiments.
(**C**) WT C2C12 cells were treated as in (A).
(**D**) Quantification of LC3b-II/α-Tubulin (left panels) and P-ATG16L1-S278/ATG16L1 (right panels) from (C). Upper panels: Torin1-treated cells; lower panels: rapamycin-treated cells. n = 4 independent experiments.
(**E**) WT and AMPKα DKO MEFs were pre-treated first without (-) or with (+) 991 [10 μM] (30 min) and then treated without (-) or with (+) Torin1 [100 nM] in the absence or presence of 991 for 2 hr and presence of BafA1 [1 μM].
(**F**) C2C12 cells were transiently transfected with scrambled (Scr) or AMPKα1/α2 siRNA and treated as in (E).
(**G**) Model: Activation of AMPK with compound 991 increases ULK1 P-S555 and suppresses Torin1-induced autophagy. Inactivation of mTORC1 with Torin1 reduces ULK1 P-S757 and attenuates the ability of AMPK to suppress autophagy.

Bars on graphs represent mean +/- SD (standard deviation). One-way ANOVA was performed followed by Sidak's multiple comparison post hoc tests; *$p < 0.05$; **$p < 0.01$; ***$p < 0.001$; ****$p < 0.0001$; ns, not significant.

Figure 9: Impaired reactivation of mTORC1 signaling during prolonged amino acid deprivation in AMPKα1/α2 double knockout/down cells

(**A**) WT and AMPKα DKO MEFs were fed with complete media (+) for 1 hr or amino acid-free media (-) for 0.5, 2, or 4 hr. Whole cell lysates were immunoblotted as indicated.
(**B**) Quantification of P-S6K1-T389/S6K1 (upper panels) and P-ULK1-S757/ULK1 (lower panels) from (A). n = 6 independent experiments.
(**C**) WT and AMPKα DKO HeLa cells (CRISPR clone #16) were treated as in (A).
(**D**) Quantification of P-S6K1-T389/S6K1 (upper panels) and P-ULK1-S757/ULK1 (lower panels) in (C). n = 6 independent experiments.
(**E**) Quantification of P-ULK1-S555 to ULK1 in MEFs (left panel) or C2C12 cells (right panel) cultured in complete media (+) or amino acid-free media (-) for 2 hr. n = 5 independent experiments.
(**F**) Quantification of P-ULK1-S555/α-tubulin in MEFs (left panel) or C2C12 cells (right panel) cultured in complete media (+) or amino acid-free media (-) for 2 hr. Note that we also normalized P-ULK-S555 to α-tubulin due the extensive shifting that ULK1 undergoes on SDS-PAGE in response to amino acid levels (likely due to phosphorylation), rendering it difficult to assess total ULK1 levels accurately. n = 5 independent experiments.
(**G**) WT and AMPKα DKO MEFs were fed with complete media (CM) for 1 hr or amino acid-free media (-) for 50 min and stimulated without (-) or with (+) amino acids for 10 min.
(**H**) WT and AMPKα DKO MEFs were amino acid-deprived (-) (50 min), pre-treated with Torin1 [100 nM] (30 min), and stimulated without (-) or with (+) amino acids (10 min).

Bars on graphs represent mean +/- SD (standard deviation). Student's t-tests (unpaired) were performed; *$p < 0.05$; ****$p < 0.0001$; ns, not significant.

Figure 10: Models

(**A)** Both mTORC1 and AMPK suppress autophagy. In amino acid-replete media, mTORC1 phosphorylates ULK1 on S757 while AMPK phosphorylates ULK1 on S555 (and likely other sites) to suppress the activity of the ULK1 complex. AMPK also suppresses the acidification of lysosomes. The inactivation of mTORC1 by amino acid withdrawal or Torin1 treatment reduces AMPK-mediated inhibitory phosphorylation of ULK1. These events contribute to the activation of the ULK1 complex, which initiates the formation of autophagosomes. During prolonged amino acid deprivation, autophagic proteolysis by autolysosomes releases free amino acids, which reactivates mTORC1 in a manner dependent on AMPK, in part. Activation of AMPK pharmacologically (e.g., with compound 991) or by glucose withdrawal suppresses autophagy.
(**B**) mTORC1-mediated phosphorylation of ULK1 during amino acid sufficiency stabilizes the AMPK-ULK1 complex. In complete media, active mTORC1 phosphorylates ULK1 S757, which stabilizes the AMPK-ULK1 interaction and thus facilitates AMPK-mediated phosphorylation of ULK1, e.g., on S555. These events inactivate the ULK1 complex. Upon amino acid withdrawal or Torin1 treatment, dephosphorylation of ULK1 S757 destabilizes the AMPK-ULK1 interaction, thus reducing AMPK-mediated phosphorylation of ULK1. These events activate the ULK1 complex.
(**C)** Different effects of AMPK on mTORC1 signaling depending on cellular context. During energetic stress, AMPK inhibits mTORC1 signaling and thereby suppresses anabolic metabolism, which improves cellular bioenergetics and promotes cell survival. During nutrient stress caused by amino acid deprivation, however, AMPK supports mTORC1 signaling, which supports essential metabolic processes.

Figure 1

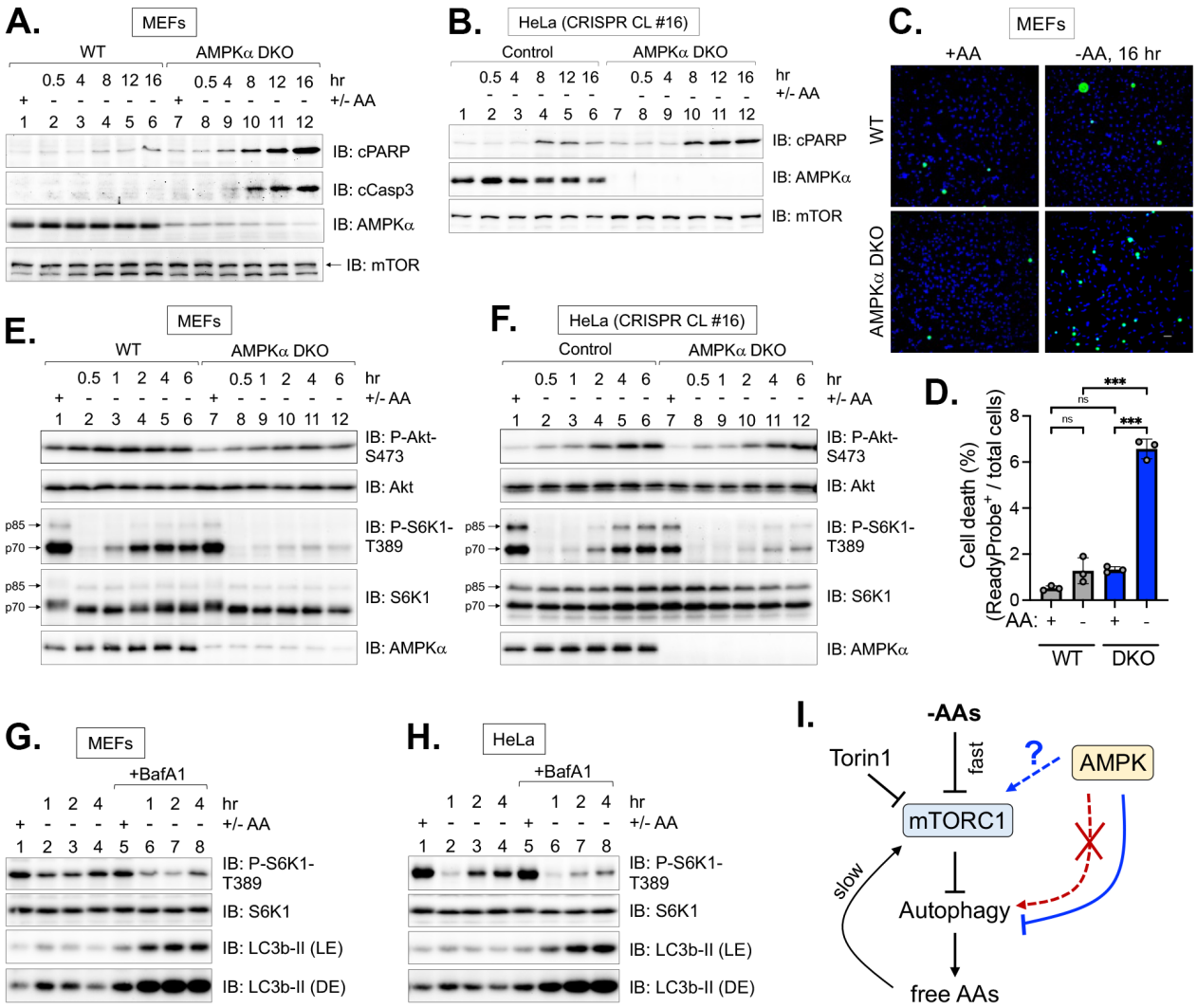
A.
MEFs
WT
AMPKα DKO
0.5 4 8 12 16 0.5 4 8 12 16 hr
+ - - - - - + - - - - - +/- AA
1 2 3 4 5 6 7 8 9 10 11 12
IB: cPARP
IB: cCasp3
IB: AMPKα
IB: mTOR
B.
HeLa (CRISPR CL #16)
Control
AMPKα DKO
0.5 4 8 12 16 0.5 4 8 12 16 hr
- - - - - - - - - - - - +/- AA
1 2 3 4 5 6 7 8 9 10 11 12
IB: cPARP
IB: AMPKα
IB: mTOR
C.
MEFs
+AA
-AA, 16 hr
WT
AMPKα DKO
E.
MEFs
WT
AMPKα DKO
0.5 1 2 4 6 0.5 1 2 4 6 hr
+ - - - - - + - - - - - +/- AA
1 2 3 4 5 6 7 8 9 10 11 12
IB: P-Akt-S473
IB: Akt
p85
p70
IB: P-S6K1-T389
IB: S6K1
IB: AMPKα
F.
HeLa (CRISPR CL #16)
Control
AMPKα DKO
0.5 1 2 4 6 0.5 1 2 4 6 hr
+ - - - - - + - - - - - +/- AA
1 2 3 4 5 6 7 8 9 10 11 12
IB: P-Akt-S473
IB: Akt
IB: P-S6K1-T389
IB: S6K1
IB: AMPKα
D.
Cell death (%)
(ReadyProbe+ / total cells)
ns
***
AA: + - + -
WT
DKO
G.
MEFs
+BafA1
1 2 4 1 2 4 hr
+ - - - + - - - +/- AA
1 2 3 4 5 6 7 8
IB: P-S6K1-T389
IB: S6K1
IB: LC3b-II (LE)
IB: LC3b-II (DE)
H.
HeLa
+BafA1
1 2 4 1 2 4 hr
+ - - - + - - - +/- AA
1 2 3 4 5 6 7 8
IB: P-S6K1-T389
IB: S6K1
IB: LC3b-II (LE)
IB: LC3b-II (DE)
I.
-AAs
Torin1
fast
?
AMPK
mTORC1
slow
Autophagy
free AAs

Figure 2

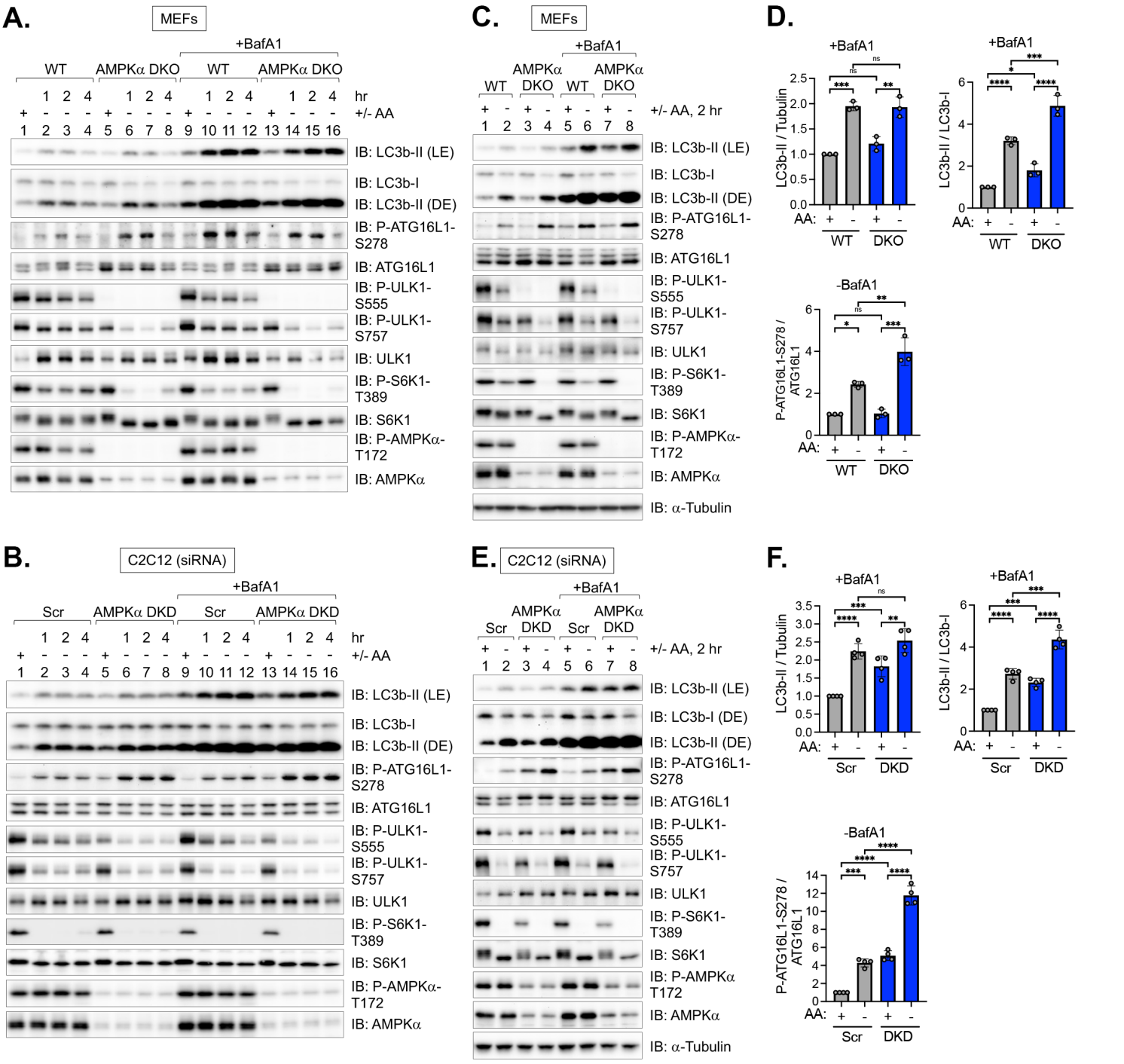
A.
MEFs
+BafA1
WT
AMPKα DKO
WT
AMPKα DKO
hr
+/- AA
IB: LC3b-II (LE)
IB: LC3b-I
IB: LC3b-II (DE)
IB: P-ATG16L1-S278
IB: ATG16L1
IB: P-ULK1-S555
IB: P-ULK1-S757
IB: ULK1
IB: P-S6K1-T389
IB: S6K1
IB: P-AMPKα-T172
IB: AMPKα
C.
MEFs
+BafA1
WT
AMPKα DKO
WT
AMPKα DKO
+/- AA, 2 hr
IB: LC3b-II (LE)
IB: LC3b-I
IB: LC3b-II (DE)
IB: P-ATG16L1-S278
IB: ATG16L1
IB: P-ULK1-S555
IB: P-ULK1-S757
IB: ULK1
IB: P-S6K1-T389
IB: S6K1
IB: P-AMPKα-T172
IB: AMPKα
IB: α-Tubulin
D.
+BafA1
LC3b-II / Tubulin
LC3b-II / LC3b-I
AA:
WT
DKO
-BafA1
P-ATG16L1-S278 / ATG16L1
B.
C2C12 (siRNA)
+BafA1
Scr
AMPKα DKD
Scr
AMPKα DKD
E.
C2C12 (siRNA)
+BafA1
Scr
AMPKα DKD
Scr
AMPKα DKD
F.
+BafA1
LC3b-II / Tubulin
LC3b-II / LC3b-I
Scr
DKD
-BafA1
P-ATG16L1-S278 / ATG16L1
G.
MEFs (-BafA1)
WT
AMPKα DKO
IB: p62
IB: α-Tubulin
H.
C2C12 (siRNA; -BafA1)
Scr
AMPKα DKD
IB: p62
IB: α-Tubulin

Figure 3

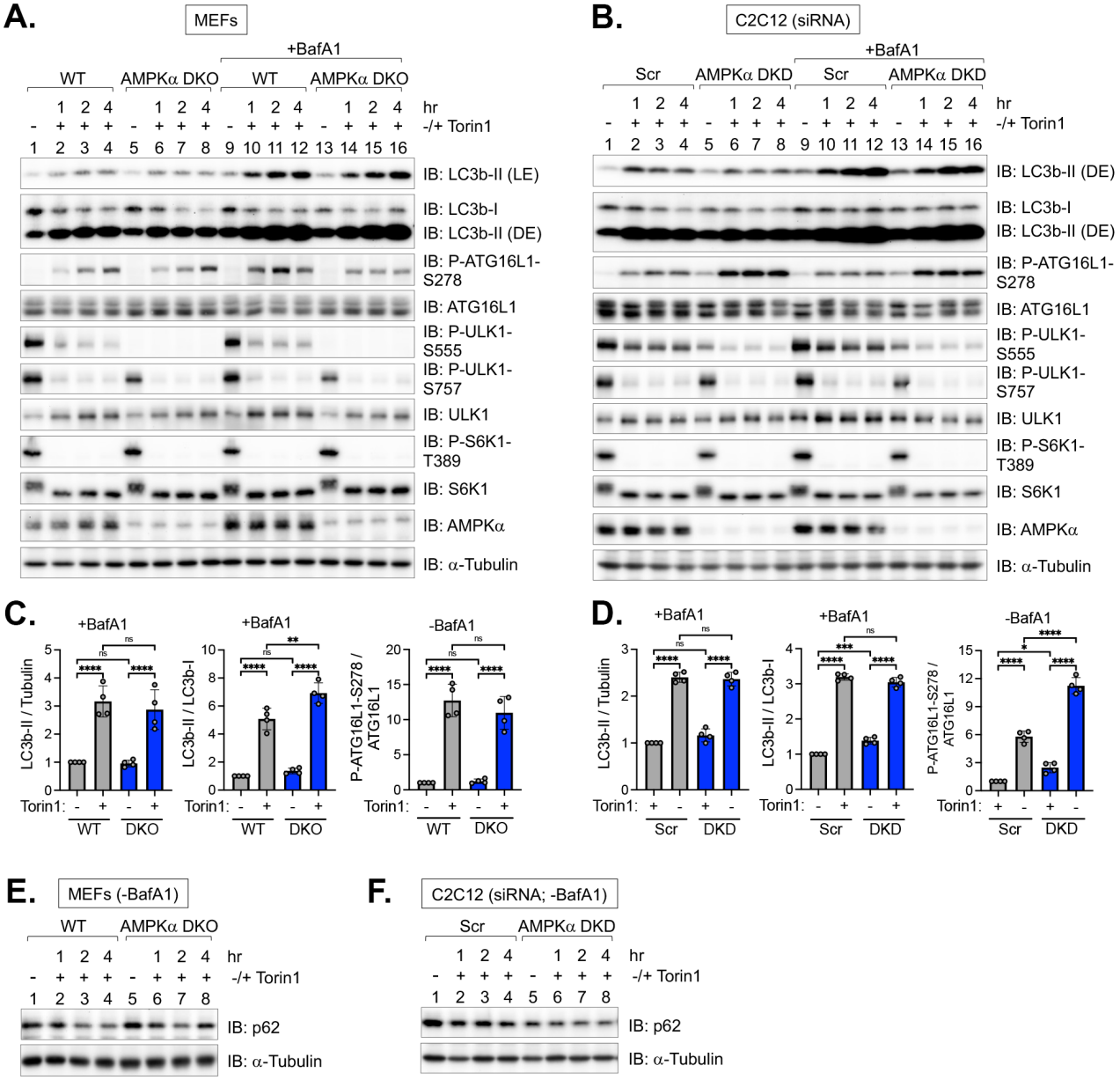
A.
MEFs
+BafA1
WT
AMPKα DKO
WT
AMPKα DKO
hr
-/+ Torin1
IB: LC3b-II (LE)
IB: LC3b-I
IB: LC3b-II (DE)
IB: P-ATG16L1-S278
IB: ATG16L1
IB: P-ULK1-S555
IB: P-ULK1-S757
IB: ULK1
IB: P-S6K1-T389
IB: S6K1
IB: AMPKα
IB: α-Tubulin
B.
C2C12 (siRNA)
+BafA1
Scr
AMPKα DKD
Scr
AMPKα DKD
hr
-/+ Torin1
IB: LC3b-II (DE)
IB: LC3b-I
IB: LC3b-II (DE)
IB: P-ATG16L1-S278
IB: ATG16L1
IB: P-ULK1-S555
IB: P-ULK1-S757
IB: ULK1
IB: P-S6K1-T389
IB: S6K1
IB: AMPKα
IB: α-Tubulin
C.
+BafA1
+BafA1
-BafA1
LC3b-II / Tubulin
LC3b-II / LC3b-I
P-ATG16L1-S278 / ATG16L1
Torin1:
WT
DKO
D.
+BafA1
+BafA1
-BafA1
LC3b-II / Tubulin
LC3b-II / LC3b-I
P-ATG16L1-S278 / ATG16L1
Torin1:
Scr
DKD
E.
MEFs (-BafA1)
WT
AMPKα DKO
hr
-/+ Torin1
IB: p62
IB: α-Tubulin
F.
C2C12 (siRNA; -BafA1)
Scr
AMPKα DKD
hr
-/+ Torin1
IB: p62
IB: α-Tubulin

Figure 4

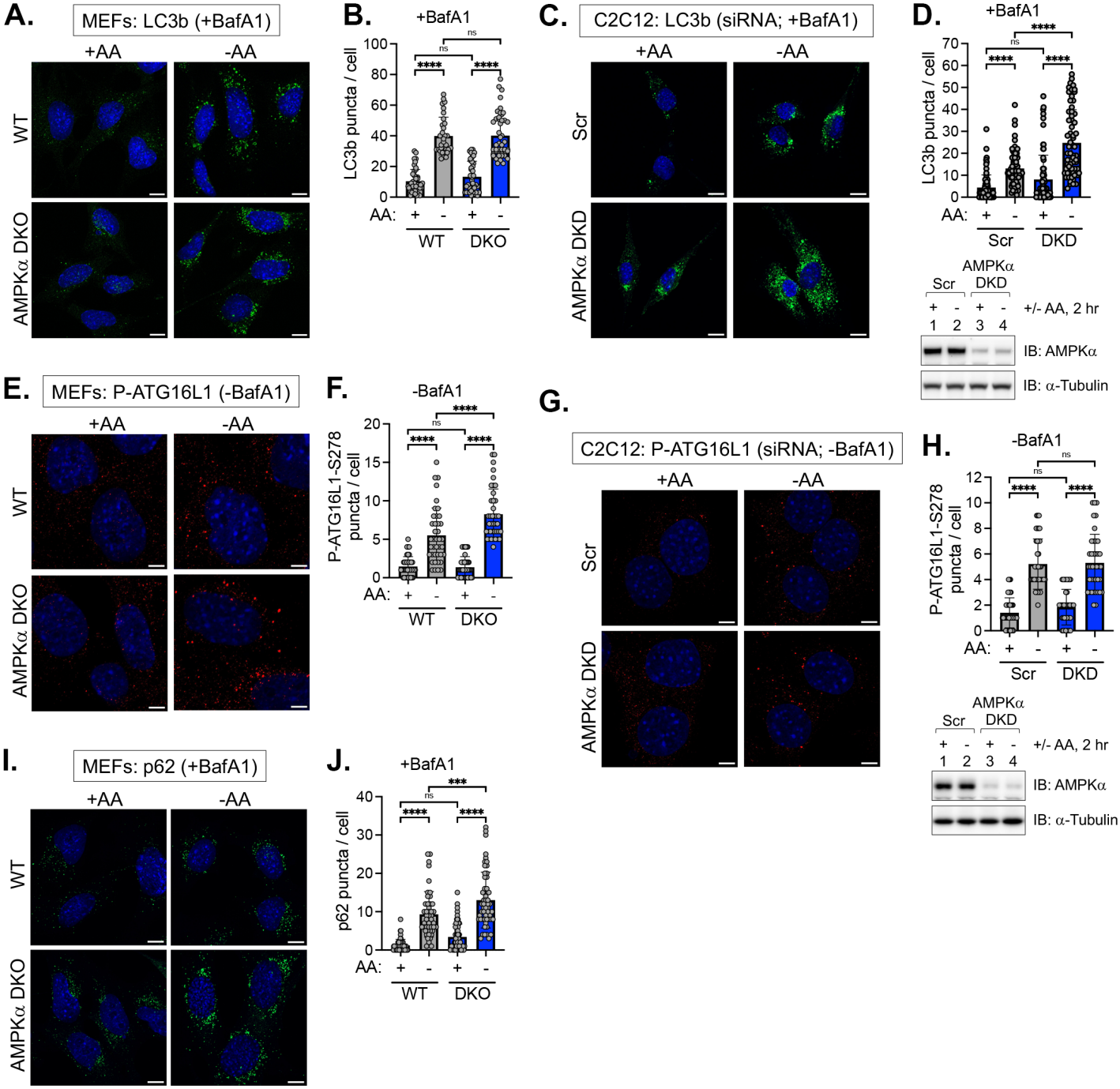
A.
MEFs: LC3b (+BafA1)
+AA
-AA
WT
AMPKα DKO
B.
+BafA1
LC3b puncta / cell
AA:
WT
DKO
C.
C2C12: LC3b (siRNA; +BafA1)
Scr
AMPKα DKD
D.
+BafA1
LC3b puncta / cell
Scr
DKD
AMPKα
+/- AA, 2 hr
IB: AMPKα
IB: α-Tubulin
E.
MEFs: P-ATG16L1 (-BafA1)
F.
-BafA1
P-ATG16L1-S278 puncta / cell
G.
C2C12: P-ATG16L1 (siRNA; -BafA1)
H.
-BafA1
P-ATG16L1-S278 puncta / cell
I.
MEFs: p62 (+BafA1)
J.
+BafA1
p62 puncta / cell

Figure 5

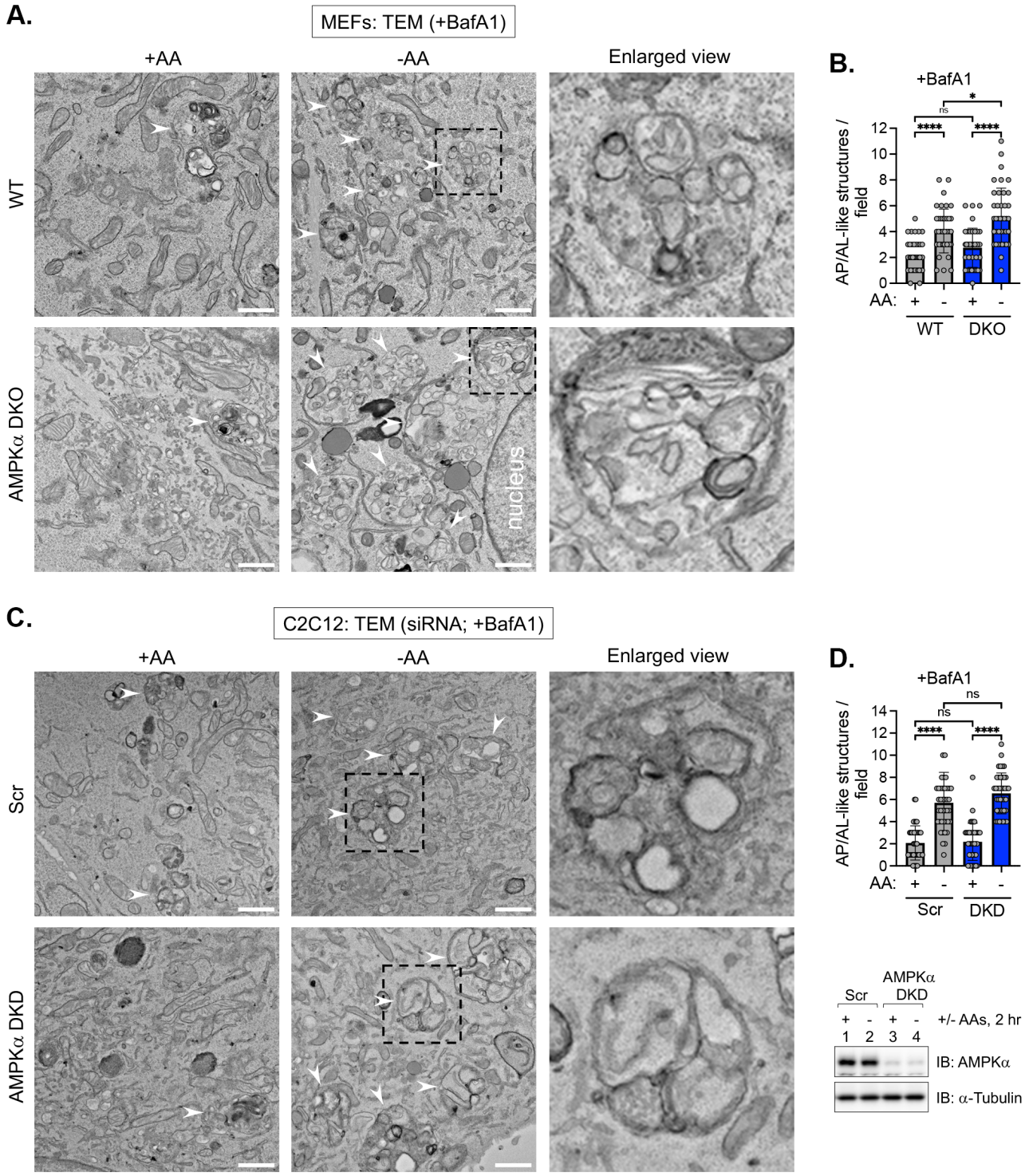
A.
MEFs: TEM (+BafA1)
+AA
-AA
Enlarged view
WT
AMPKα DKO
nucleus
B.
+BafA1
AP/AL-like structures / field
ns
*
****
****
AA:
WT
DKO
C.
C2C12: TEM (siRNA; +BafA1)
+AA
-AA
Enlarged view
Scr
AMPKα DKD
D.
+BafA1
AP/AL-like structures / field
ns
ns
****
****
AA:
Scr
DKD
AMPKα
Scr
DKD
+/- AAs, 2 hr
1 2 3 4
IB: AMPKα
IB: α-Tubulin

Figure 6

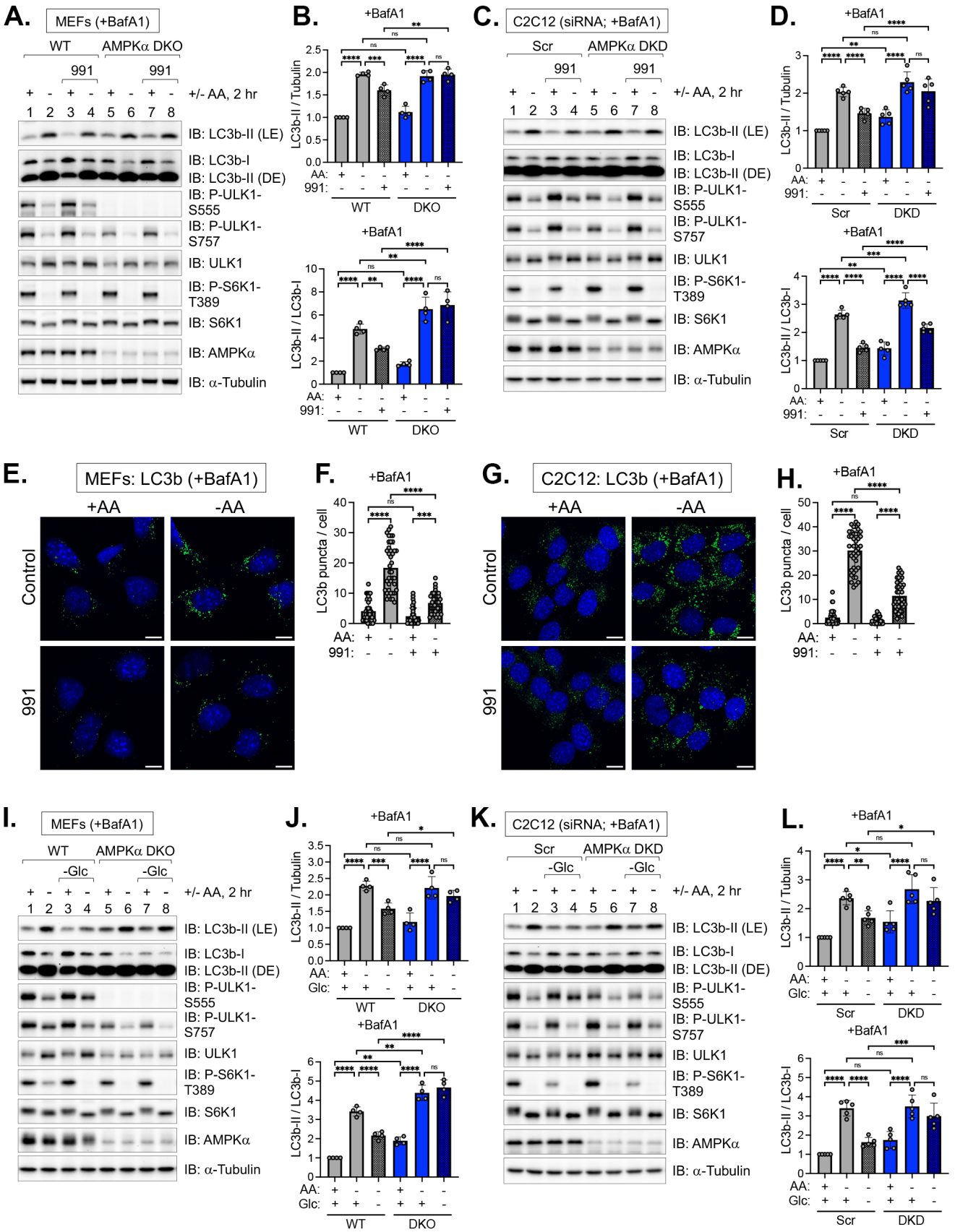
A.
MEFs (+BafA1)
WT
AMPKα DKO
991
+/- AA, 2 hr
IB: LC3b-II (LE)
IB: LC3b-I
IB: LC3b-II (DE)
IB: P-ULK1-S555
IB: P-ULK1-S757
IB: ULK1
IB: P-S6K1-T389
IB: S6K1
IB: AMPKα
IB: α-Tubulin
B.
+BafA1
LC3b-II / Tubulin
LC3b-II / LC3b-I
AA:
991:
WT
DKO
C.
C2C12 (siRNA; +BafA1)
Scr
AMPKα DKD
D.
DKD
E.
MEFs: LC3b (+BafA1)
+AA
-AA
Control
F.
LC3b puncta / cell
G.
C2C12: LC3b (+BafA1)
H.
I.
-Glc
Glc:
J.
K.
L.

Figure 7

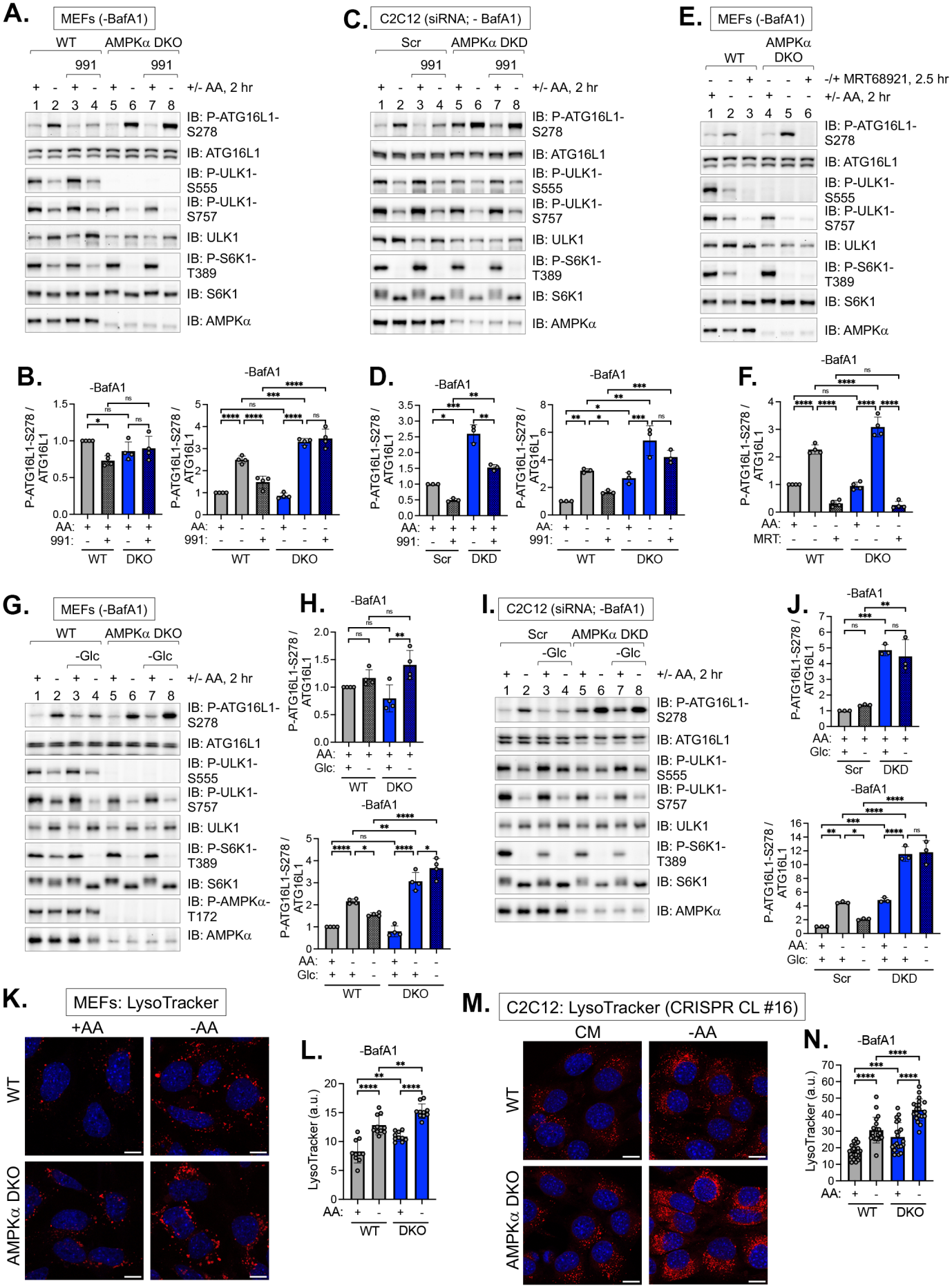
A.
MEFs (-BafA1)
WT
AMPKα DKO
991
+/- AA, 2 hr
IB: P-ATG16L1-S278
IB: ATG16L1
IB: P-ULK1-S555
IB: P-ULK1-S757
IB: ULK1
IB: P-S6K1-T389
IB: S6K1
IB: AMPKα
B.
-BafA1
P-ATG16L1-S278 / ATG16L1
AA:
991:
WT
DKO
C.
C2C12 (siRNA; - BafA1)
Scr
AMPKα DKD
D.
Scr
DKD
E.
MEFs (-BafA1)
-/+ MRT68921, 2.5 hr
F.
MRT:
G.
MEFs (-BafA1)
-Glc
IB: P-AMPKα-T172
H.
Glc:
I.
C2C12 (siRNA; -BafA1)
J.
K.
MEFs: LysoTracker
+AA
-AA
L.
LysoTracker (a.u.)
M.
C2C12: LysoTracker (CRISPR CL #16)
CM
N.

Figure 8

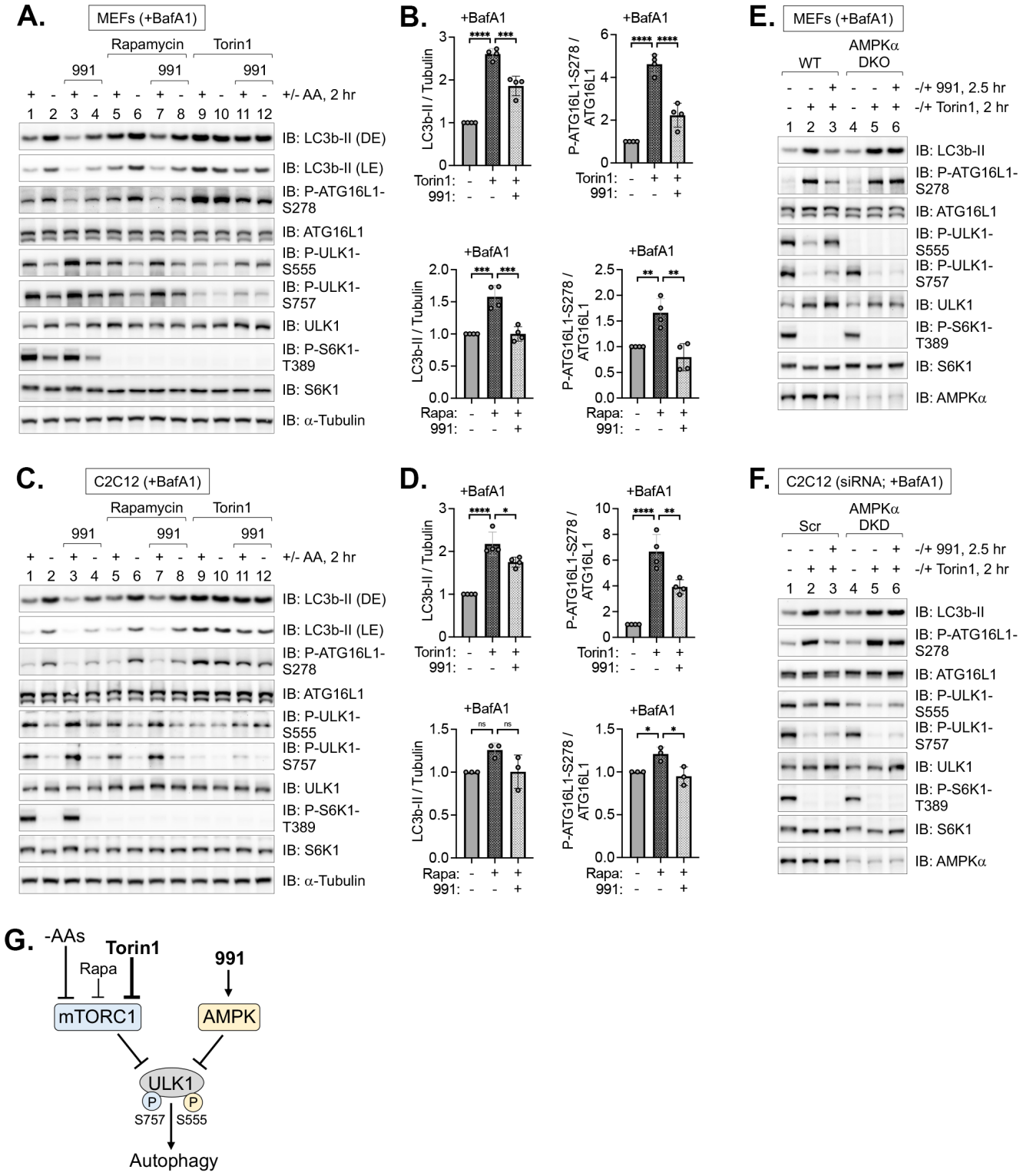
A.
MEFs (+BafA1)
Rapamycin
Torin1
991
+/- AA, 2 hr
IB: LC3b-II (DE)
IB: LC3b-II (LE)
IB: P-ATG16L1-S278
IB: ATG16L1
IB: P-ULK1-S555
IB: P-ULK1-S757
IB: ULK1
IB: P-S6K1-T389
IB: S6K1
IB: α-Tubulin
B.
+BafA1
LC3b-II / Tubulin
P-ATG16L1-S278 / ATG16L1
Torin1:
Rapa:
991:
C.
C2C12 (+BafA1)
D.
E.
MEFs (+BafA1)
WT
AMPKα DKO
-/+ 991, 2.5 hr
-/+ Torin1, 2 hr
F.
C2C12 (siRNA; +BafA1)
Scr
AMPKα DKD
G.
-AAs
Rapa
Torin1
991
mTORC1
AMPK
ULK1
P
S757
S555
Autophagy

Figure 9

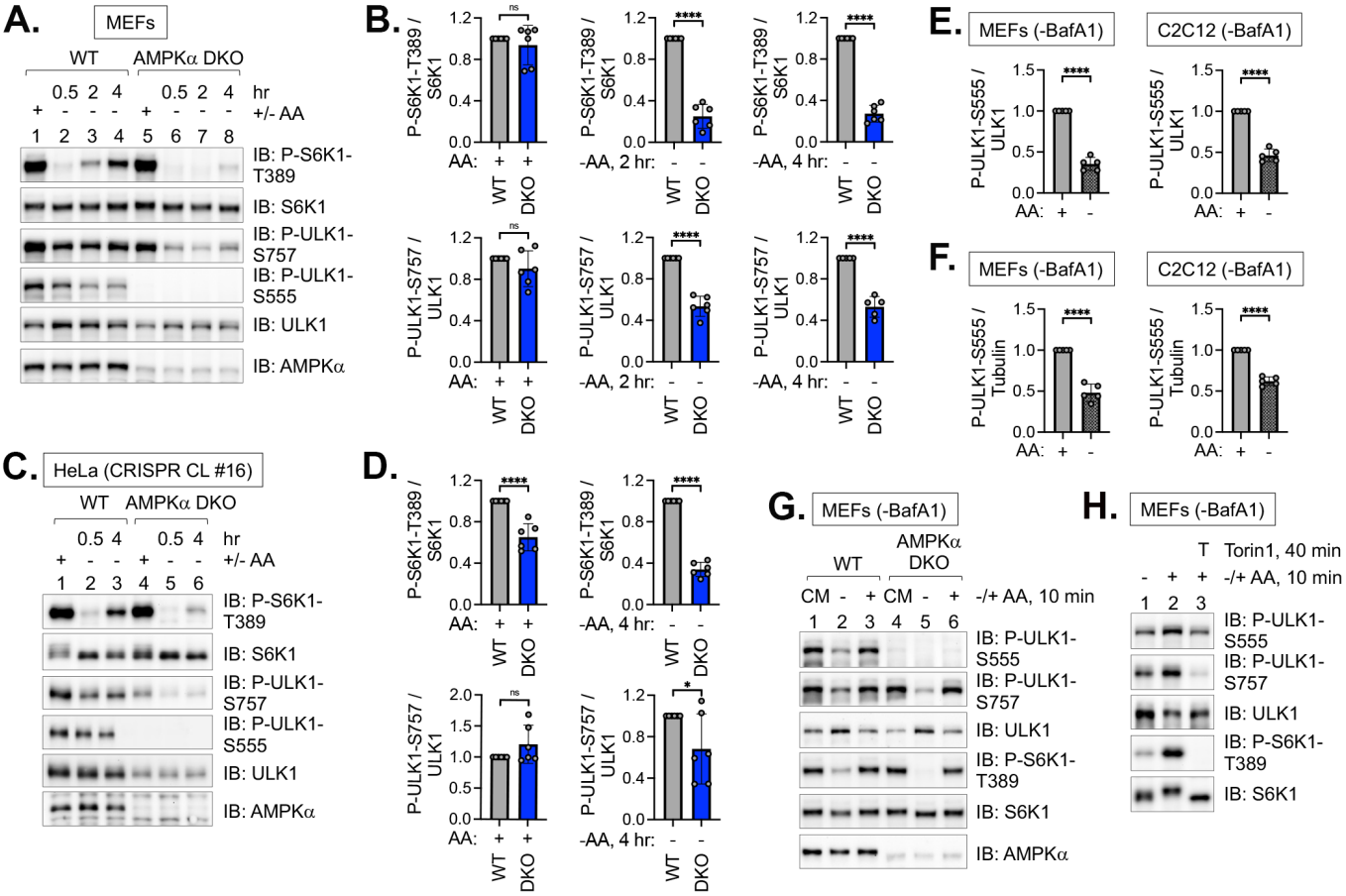
A.
MEFs
WT
AMPKα DKO
0.5 2 4
0.5 2 4
hr
+/- AA
1 2 3 4 5 6 7 8
IB: P-S6K1-T389
IB: S6K1
IB: P-ULK1-S757
IB: P-ULK1-S555
IB: ULK1
IB: AMPKα
B.
P-S6K1-T389 / S6K1
P-ULK1-S757 / ULK1
AA:
-AA, 2 hr:
-AA, 4 hr:
WT
DKO
ns
****
C.
HeLa (CRISPR CL #16)
WT
AMPKα DKO
0.5 4
0.5 4
hr
+/- AA
1 2 3 4 5 6
IB: P-S6K1-T389
IB: S6K1
IB: P-ULK1-S757
IB: P-ULK1-S555
IB: ULK1
IB: AMPKα
D.
P-S6K1-T389 / S6K1
P-ULK1-S757 / ULK1
AA:
-AA, 4 hr:
WT
DKO
ns
****
*
E.
MEFs (-BafA1)
C2C12 (-BafA1)
P-ULK1-S555 / ULK1
AA:
****
F.
MEFs (-BafA1)
C2C12 (-BafA1)
P-ULK1-S555 / Tubulin
AA:
****
G.
MEFs (-BafA1)
WT
AMPKα DKO
CM - + CM - +
-/+ AA, 10 min
1 2 3 4 5 6
IB: P-ULK1-S555
IB: P-ULK1-S757
IB: ULK1
IB: P-S6K1-T389
IB: S6K1
IB: AMPKα
H.
MEFs (-BafA1)
T Torin1, 40 min
- + + -/+ AA, 10 min
1 2 3
IB: P-ULK1-S555
IB: P-ULK1-S757
IB: ULK1
IB: P-S6K1-T389
IB: S6K1

Figure 10

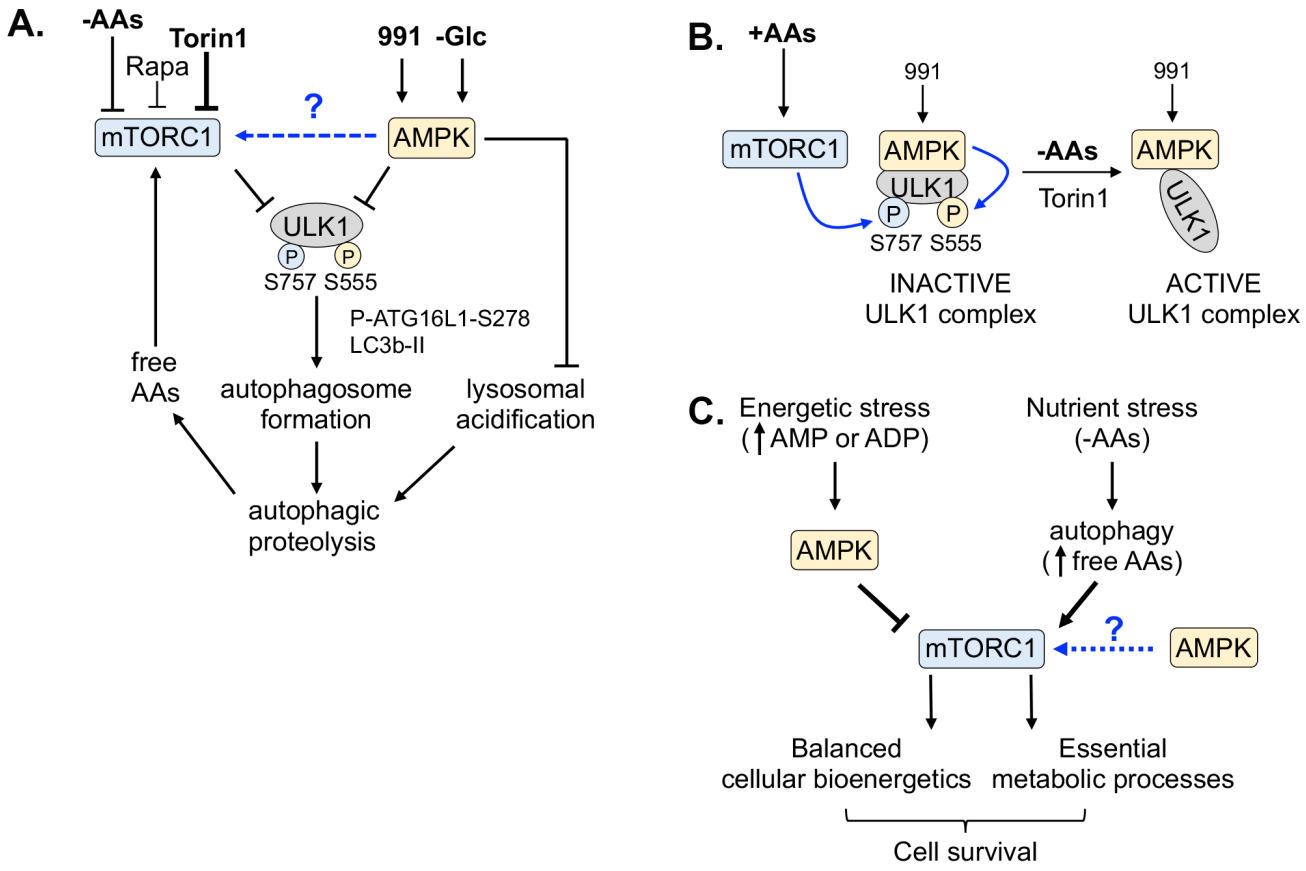
A.
-AAs
Torin1
Rapa
991
-Glc
?
mTORC1
AMPK
ULK1
P
P
S757 S555
P-ATG16L1-S278
LC3b-II
free
AAs
autophagosome
formation
lysosomal
acidification
autophagic
proteolysis
B.
+AAs
991
991
mTORC1
AMPK
ULK1
P
P
S757 S555
-AAs
Torin1
AMPK
ULK1
INACTIVE
ULK1 complex
ACTIVE
ULK1 complex
C.
Energetic stress
(↑AMP or ADP)
Nutrient stress
(-AAs)
AMPK
autophagy
(↑free AAs)
mTORC1
?
AMPK
Balanced
cellular bioenergetics
Essential
metabolic processes
Cell survival